Modeling the Effect of Non-Spherical Particle Size in Laser Metal Deposition Process

NS Amna Liaqat
00000172417

Supervisor

Dr. Khalid Mahmood

Department of Mechanical Engineering

Collage of Electrical and Mechanical Engineering (CEME)
National University of Science and Technology (NUST)
Rawalpindi

MARCH 2019

Modeling the effect of Non-Spherical Particle Size in Laser Metal Deposition Process

NS Amna Liaqat
Registration # 00000172417

A thesis submitted in partial fulfillment of the requirements for the degree of MS Mechanical Engineering

Supervisor

Dr. Khalid Mahmood

Supervisor´s Signature:____

Department of Mechanical Engineering

Collage of Electrical and Mechanical Engineering (CEME)
National University of Science and Technology (NUST)
Rawalpindi

MARCH 2019

DECLARATION

I certify that this research work titled **"Modeling the Effect of Non-Spherical Particle Size in Laser Metal Deposition Process"** is my own work. The work has not been presented elsewhere for assessment. The material that has been used from other sources has been properly acknowledged / referred.

Signature of Student
NS Amna Liaqat
00000172417

LANGUAGE CORRECTNESS CERTIFICATE

This thesis has been read by an English expert and is free of typing, syntax, semantic, grammatical and spelling mistakes. Thesis is also according to the format given by the university.

Signature of Student
NS Amna Liaqat
00000171143

Signature of Supervisor
(Dr Khalid Mahmood)

ACKNOWLEDGEMENTS

First of all I am grateful to ***ALLAH***, who has given me guidance, strength and enabled me to accomplish this task. The journey on this road of success had not been possible without His will, and henceforth, all this success and accomplishment, I owe it to Him, in totality.

I want to thank my Parents for their support and prayers. They have been a driving force and without their support I might not have been able to get done with my thesis.I am grateful to my siblings, friends and well-wishers for their untiring support.

I would like to express immense gratitude to my supervisor ***Dr Khalid Mahmood***, for his help and motivation throughout this journey of completing my research work. Without his help I would have not been able to accomplish this tedious job. Under his guidance, I am able to achieve my goals. He helped me throughout this journey of research and I'm really grateful for his unfailing support and assistance throughout my work.

I would like to thank my GEC member ***Dr Imran Akhter*** for his willingness to offer me his time and intellect during my research.

I would like to thank my GEC member ***Dr Raja Aamer***, for broadening my concepts and guideline about research outline.

DEDICATION

I dedicate this work to my Parents and Siblings for their support, love and guidance. I appreciate their encouragement during all phases of my research and studies.

ABSTRACT

Additive manufacturing (AM) is the standardized name to describe the new world of manufacturing technology that built 3D objects by adding materials in layers, whether the material is in plastic, ceramics, metal and or it is advancing towards human tissues.AM can also be described as rapid manufacturing (RM). AM processes needs only few basic dimensional details, understanding of AM machines and building material that could be used to manufacture the part. Laser metal deposition (LMD) is form of AM, a method that has a great possibility to reduce material waste through near net shape production as well as adding value to an already manufactured costly component (aviation and aerospace industry). Laser Metal deposition (LMD) process offers the potential to make a metallic component directly from CAD file. The focus of this study is an investigation of powder stream process, a sub process of LMD. Powder stream and processing parameters are highly important in clad formation, it directly affect powder distribution, temperature attenuation of beam and velocity during LMD. Various Modeling techniques have been used to model this sub process such as: dimensional modeling, statistical modeling and a review of analytical Modeling has been done. Effect of different processing parameters on clad height, clad width and surface hardness has been studied. The results of these investigations have also been validated with an experimental work.

TABLE OF CONTENTS

LIST OF TABLES

LIST OF FIGURES

LIST OF ACRONYMS

3D	Three Dimensional
.stl	Standard File Format for 3D Printing
AM	Additive Manufacturing
ANOVA	Analysis of Variance
ANN	Artificial Neural Network
CAD	Computer Aided Design
CCD	Central Composite Design
DoE	Design of Experiments
EDS	Energy Dispersive x-ray Spectroscopy
FEA	Finite Element Analysis
FEM	Finite Element Method
LF	Large Fragment
LMD	Laser Metal Deposition
RP	Rapid Prototyping
RM	Rapid Manufacturing
RSM	Response Surface Methodology
RCBD	Randomized Complete Block Design
SF	Small Fragment

Chapter 1

INTRODUCTION

1.1 Research Background

Laser metal deposition (LMD) is the form of Additive Manufacturing (AM), a method that has a great possibility to reduce material waste through near net shape production as well as adding value to an already manufactured costly component. LMD process offers the ability to make a metal component directly from the CAD file. Various Materials including ferrous, nonferrous, polymer and ceramics can be used. The process can utilize the commercially available powder in the industry that already exists in a wide variety [1].

The process is well known by many names, these include Laser Engineered Net Shaping, Laser Cladding, Laser Deposition Welding, and Powder Fusion Welding. This technique has shown enormous possibility for different fields such as part repairing and rapid manufacturing, etc. [2-4].

An essential advantage of LMD over other conventional methods is the relatively low heat that is applied during the process. The high level of control over the laser beam means that precise amounts of energy can be applied to the critically defined regions of the substrate. As a result, this process creates much less damage by heat or deformation to the part. Apart from this, a fine and improved microstructure can be achieved. As the laser beam tends to be more stable and easily adjusted, the process is highly consistent leading to much higher reliability. Process automation is also very easy and understandable, and material build-up rates are high, leading to controlled and fast processing speeds and that’s how it found application in aviation, aerospace, medical and automotive industry [5].

Typical application of this process comes for the repair of costly components such as turbine parts and the repair of critical tools. In order to use this method on large scale and in industries such as aerospace and others, advancement in modeling methods is required that helps to study the more precise and controlled effect of processing parameters [6]. Modeling has become an important tool to evaluate or check the quality of the final product by considering the processing parameters. Accurate and precise modeling processes can pinpoint any defect in the process and can help to establish a logical process control relations. Investigation of all the processing parameters with conventional manufacturing processes would be very time consuming and costly so modeling has become an important and necessary tool to lessen the number of manufacturing trials which are needed. Many research papers have been published on modeling the LMD process by dividing the whole process in sub processes. Different modeling techniques including empirical, dimensional, analytical and numerical have been used to study the effects of different processing parameters for optimized results. A comparison is needed between these modeling techniques and experimental data for better understanding of process control.

1.2 Aims and Objectives

The focus of this study is to investigate the effect of processing parameters on the geometric features of clad by keeping particle morphology with size variations in mind. The focus of the research to achieve this are as following:

- Investigation of the powder stream process in LMD
- Dimensional modeling of clad geometry by considering the influence of processing parameters.
- Statistical modeling of clad geometry.
- A brief analytical study of powder morphology effect on clad geometry with future suggestions

1.3 Thesis Outline

The thesis comprises of six chapters. The outline of the thesis structure is as under:

- Chapter 1. This chapter covers the research background, the aim and objectives of the research.
- Chapter 2. This chapter covers the literature review pertaining to AM processes in details, LMD process, processing parameters that affect the clad geometry in LMD process, advancement in modeling techniques, Dimensional, statistical and analytical modeling techniques and application of LMD processes.
- Chapter 3. This chapter covers the dimensional modeling of clad height in response of processing parameters.
- Chapter 4. This chapter covers the statistical modeling of processing parameters used in LMD.
- Chapter 5. This chapter covers a brief study of analytical modelling review of powder stream flow in LMD process.
- Chapter 6. Conclusions drawn from the work are summarized in this chapter. Recommendations about future work in this area have also been included in this chapter.

Chapter 2

LITERATURE REVIEW

2.1 Additive Manufacturing (AM)

AM is gaining attention from recent years due to increased technological development and reduction in time and effort [7]. AM technologies with research history of about 40 years are being deployed commercially to address the rising international competition in manufacturing lane. AM techniques are advancing in the field of medicine and orthopaedic [8]. Conversely to a material subtraction processes like CNC machining AM is layer by layer material addition process using heating source, independent of complexity and cost of final parts,only some basic dimensional details and understanding of how the AM machine works and the know-how of building materials that are used to manufacture the part [9]. Regardless of the typical feature of layer by layer addition of material, AM differ in its techniques to build the final part. Some of its techniques can consist of powder that already placed and production of parts through selective laser sintering (SLS) [10] or metallic powder can be injected through laser metal deposition (LMD) [11]. LMD is main method of AM where powder becomes in contact with laser beam while depositing, melting with the energy of laser power and making a melt pool on the substrate [12]. Illustration of SLS and LMD processes has been illustrated in Fig 2.1.

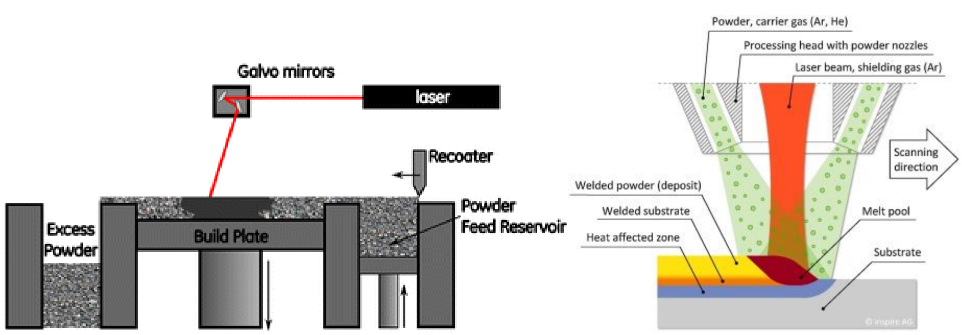

Figure 2-1 Illustration of Different AM Processes: (a) SLS [13], (b) LMD [14]

2.1.1 Generic AM Processes

Generic AM process are as follow:

- Making of CAD file in computer
- Conversion to STL format
- Transfer that file to AM Machine in form of G-code
- Setup of AM Machine
- Building of Part
- Removal from the machine
- Post processing of the built component
- Application

2.2 Laser Metal Deposition (LMD)

LMD processes permit the creation of components by first melting the material as it is being deposited through a deposition head shown in Fig 2.3. LMD is suitable for ceramics, polymers and metal composites but is mainly used for metallic powders.

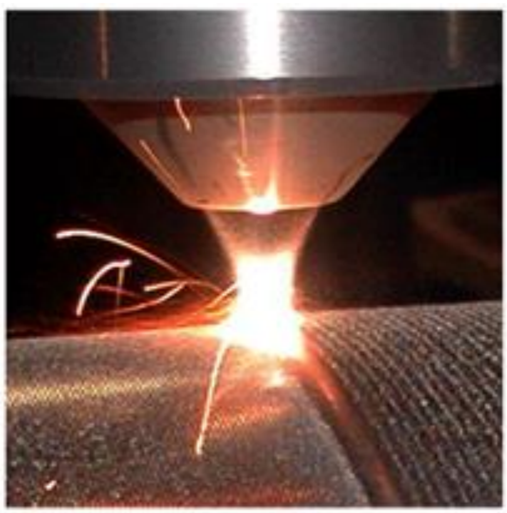

Figure 2-2 LMD Process [15]

Main subsystems involve in LMD process are listed below

- Laser (heating source)
- Material delivery system

- Traversing and shielding mechanism

2.2.1 Laser

Laser is one of the most remarkable findings of the last century and it is finding several applications in modern manufacturing. Laser is a process of optical amplification, a monochromatic and coherent electromagnetic radiations having characteristics of higher intensity. Word LASER is an acronym of "Light Amplification by Simulated Emission of Radiation" [16].

For heating, laser is required to carry adequate amount of thermal heat to cause the powder to melt in a very controlled manner without creating much heat effected zone, so that the molten material speedily solidifies again [1]. Most commonly used lasers in LMD processes are carbon dioxide (CO_2) laser, Nd: YAG laser, diode laser, fiber laser [6].

2.2.2 Material Delivery

In LMD material can be delivered to melt pool in the form of metallic powder, wires and in a combination of them. The powder particles can have different morphology and sizes.

2.2.2.1 Powder Feeding and Delivery

Powder form is the most accomplished feedstock material as most of the metal and ceramic materials are conveniently available in powder form. Metallic powders are fed through a system that should have characteristics of continuous material supply at desired levels. There are many kinds of powder feeders available according to the working feasibility. It can be hoppers [17] gravity-fed powder feeder [18] and vibratory powder feeder [19]. During the process, not all the powder is covered in the melt pool, so to recapture excessive amount of powder there should be some system that can collect it in clean form. In LMD, the main factor in the laser beam is the energy density that should be certainly above a critical amount to make melt pool as shown in Fig 2.3.

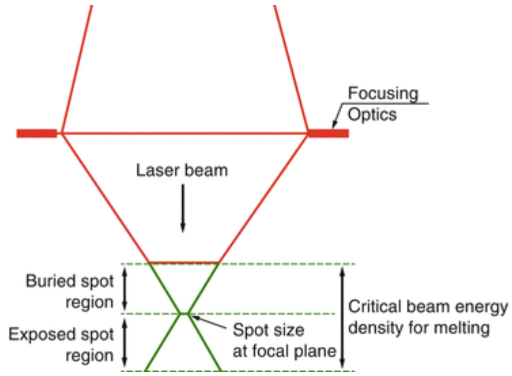

Figure 2-3 Schematic of Laser Power Density Distribution [1]

As material delivery of powder is done by nozzle so different configurations of nozzles can be used according to complexity of process, Fig 2.4 illustrate different nozzle arrangements classified as:

- Coaxial Nozzle Feeding
- Multi Axis Nozzle

Coaxial Nozzle: In coaxial nozzle feeding, the powder particles are fed as a toroid surrounding the beam of laser, focused on a narrow point using inert gas shielding to eliminate contamination [21] [22].

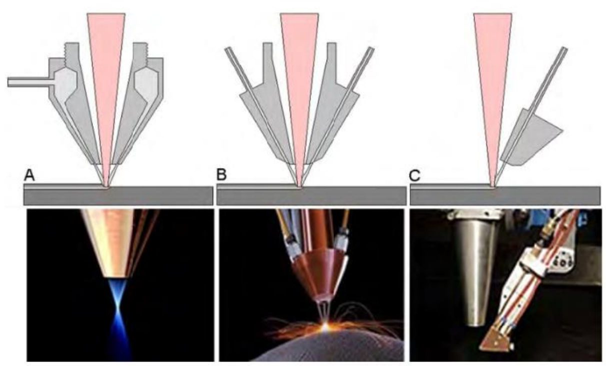

Figure 2-4 A: Coaxial Nozzle, B: Multiple Stream Flow Nozzle, C: Single Feeding Nozzle [20]

The main advantage of coaxial nozzle is that it is independent of motion of deposition head.

Multi Axis Nozzle:

It involves the introduction of powder stream through multi axis to the laser source. Single lateral nozzle converged at an intersecting point between laser beam and the substrate. Multi axis nozzle involves equally spaced multiple nozzle heads, concentrated at the melt pool. The lateral nozzle has usually a perfect circular outlet when it comes to reach at complex points [23].

2.2.2.2 Wire Feeding

In wire feeding, there is 100 % feedstock material capture efficiency; volume deposited is always equal to the total wire volume that fed during process. Wire feeding has grabbed less attention due to the lack of making complex end parts [24]. Wires are mostly in use for simple and “blocky” geometries without many complex transitions.

2.2.3 Shielding and Traversing

Shielding is normally provided by inert gasses to avoid oxidation during the LMD process. Helium [25], Argon [26] and Nitrogen [27] have been used by researchers.

2.3 LMD Processing Features

2.3.1 Build Material

LMD processes aim to create 3D end products. Powder materials or powder which are stable in the molten pool, can be utilize for the production of parts. Although material can be used both in powder and wire form but powder is generally a choice. It has an advantage of adjusting the clad dimension as required. In general, metals with high thermal conductivities and reflectivities such as aluminum alloys and gold are difficult to process during LMD [1].

Metallic materials that shows good weldability are reasonable to process. Powder is processed from metals and ceramics. Powder of traditional ceramics naturally found (clay, quartz) produced by crushing and grinding. Gas atomized (GA) metal powder has been in use when it comes to LMD as it produces spherical shape powder particles [28]. Water atomized (WA) is another cheap method of producing powder particles but they can deviate from their spherical shape [29].

2.3.2 Processing Parameters

The variables in the form of processing parameters affect the quality of laser deposition process. A careful selection is required to get desired results. Following are crucial processing parameters:

- Powder mass flow rate
- Laser power
- Scanning speed
- Beam diameter

Powder Mass Flow Rate: It is the amount of material supplied per unit time. It effect the dimensional accuracy of the deposited layer as well as the mechanical properties of the final product [30].

Laser Power: It is the main source of energy to melt the deposited material and affects the dynamics of melt pool. Many laser types can be used in LMD process. Main difference in different types of laser power is in their wavelength, as wavelength increases absorption of laser energy for most of the metals decreases [31].

Beam Diameter: it determines the spot diameter of laser that consequently tell the width of deposited layer [32].

Scanning Speed: It is the speed of laser source as it traverses, or if the laser source is stationary it is the speed of substrate with which it is moving. It affects the solidification time and deposited material quantity [33].

Many other processing parameters accounted for LMD are listed below:

- Injection Angle
- Geometry of Nozzle
- Carrier Gas Flow Rate
- Powder Feed Rate
- Microstructure
- Residual Stress

- Cracking
- Preheating process of the Powder
- Standoff distance

2.4 Effect of processing parameters

2.4.1 Powder Size and Morphology

Following are the main features regarding powder particles.

- Particle Size
- Particle Shape and Structure

Particle size involves the dimensions of the individual powder particles. To measure particle size different methods can be employed. Most common method uses the screen of different mesh sizes [34] as shown in Fig 2.5. Determination of particle size by sieving method is one of the traditional methods to measure size of the particle. Practically, a stack of decreasing mesh size sieves bottom is mechanically tremble. Depending on the mesh size particles sizes are determined.

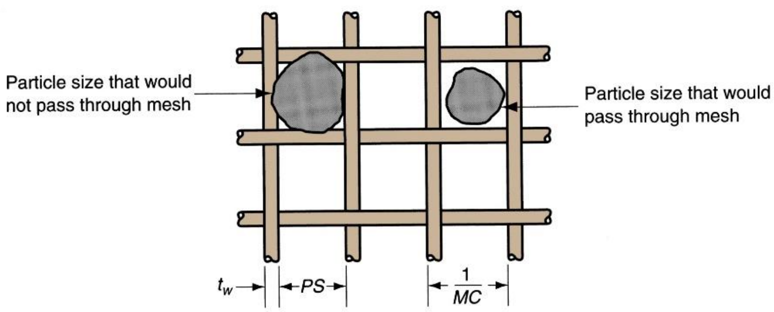

Figure 2-5 Mesh of Different Sizes to Measure Particle Size [90]

From below formula one can measure the particle size approximately.

$$\text{Particle Size} = PS = 1/MC - t_w$$

where MC is mesh count and t_w is the wire thickness of screen mesh. Other methods such as microscopy [35] and laser x-ray diffraction [36] techniques can also be employed to measure the size of particles.

Dimension of various particle shapes can be described as:

- Spherical
- Non-spherical

To calculate spherical particle size diameter is a significant factor. For measuring the non-spherical size aspect ratio can be employed to get approximate results. It was found that particle shapes can be divided into three basic categories, Particles are referred to as spherical and near-spherical and non-spherical particles, which can be sub classified into regular satellite/elongated and irregular. The deviation from pure spheres induces more particle dispersion, which greatly impacts the powder stream focusability at the nozzle exit [37].

Powder particles size and shape plays an important role in the LMD process in terms of deposition quality and deposition efficiency. It has been observed that as the shape of particle changes it affects the quality of the final deposited layer. As particle size increases, it attenuate laser power and energy degradation occur [38]. Change in shape and size of powder particles affect the temperature distribution of particles and finally, it affects the melt pool dynamics [39].

2.4.2 Hardness

Hardness is essential measure of plastic yield stress of a metal and it is resistance to scratch or indentation [40]. Grain size plays an important role when it comes to hardness. Hall-petch equation define this process in following equation [41].

$$H=H_0+cd^{-1/2}$$

Where c is Hall-petch coefficient and d is grain size. Hardness has an inverse relation with grain size. Hardness varies when variation observed in chemical composition of material.

2.5 Advances in LMD Modelling

There are advancements in the process of modelling the stages of the LMD process. The whole process of LMD has been commonly considered in different levels and advances in physical modeling of the different process levels are then considered. Fig 2.7 illustrates the different physical stages of LMD:

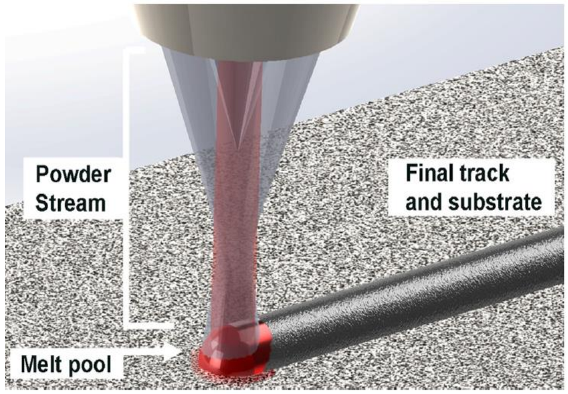

Figure 2-6 Different Physical Stages of LMD Process [42]

The process has been divided into sub processes:

- Powder Stream Processes
- Melt Pool Processes
- Final Track Microstructure

The powder stream processes are highly important for making track as LMD can be directly affected by powder distribution, beam attenuation, velocity and temperature at substrate. Various Modelling techniques have been used to model this sub process such as:

- Dimensional Modelling
- Statistical Modelling
- Analytical Modelling

2.6 Dimensional Modelling

It is a method of dimension, where physical quantities are expressed in terms of their fundamental dimensions that is often used when there is not enough information to set up precise equations. Bridgman explains it thus: "The principal use of dimensional analysis is to deduce from a study of the dimensions of the variables in any physical system, certain limitations on the form of any possible relationship between those variables. The method is of great generality and mathematical simplicity" [43]. A mathematical method has been used in investigation and technology for the design and for conducting many model tests. It works with the physical quantities involve in the model or experiment. It is a mathematical technique used to predict physical parameters and their effect in flow, heat transfer and on thermodynamic properties.

It must be emphasized that dimensional analysis is not a complete solution to a mathematical problem. It usually provides only a partial solution. The correctness of dimensional method entirely depends on how an individual using it, defining the dependent and independent parameters. If the researcher omits a crucial variable, results will be different and may lead to incorrect results [44].

Many researchers used this dimensional modeling technique and found useful results. Subodh Kumar et al. illustrate the dimensional model to study the layer height deposited using Π Backingum theorem by considering main material processing parameters and main energy processing parameters that influence the deposited layer height by LMD. The influence of laser scanning speed on layer height deposited showed that layer height decreased when scanning speed increased [45]. The suggested model can also be utilize for other two main building parameters, mass flow rate and laser power, as results of above model are in good agreement with a medium range of laser traverse velocity.

2.6.1 Applications of Dimensional Analysis

In following aspects dimensional analysis can be helpful [46]:

- To develop an equation for phenomenon where fluid flow properties are required
- To convert one system of units to another system of units
- To reduce the variables required in an experiment

2.7 Empirical and Statistical Modelling

Empirical-Statistical modeling has been in use since emerging time of laser metal deposition process. The main purpose is to avoid physical phenomenon involved in the process.

2.7.1 Design of Experiments (DoE) Techniques

DoE is a statistical method to find the relationship between input processing parameters and outcomes [47].

2.7.2 Aim of Design of Experiments

The option of a appropriate DoE technique depends entirely on the aim of the experiment. For more detailed computation where main and interactive effects needs to be considered, a fractional or a full factorial method (FFD) is better option [48]. Randomized Complete Block Design (RCBD) is a design of experiments technique based on blocking. RCBD is usually characterized by equally sized blocks; each containing all of the treatments [49]. The basic idea behind latin square is to perform one experiment in one block only so that no randomization is required. If an experiment has to perform to consider primary factors latin square or RCBD would be appropriate [50]. If error variables could influenced significant on the experiment, a Taguchi method is suitable [51]. For RSM purposes, a FFD or CCD can be chosen. In full factorial, samples could make by giving every possible combination of the factors values. It is just a clue on how to use DoE technique. When dealing with RSM both DoE technique and RSM technique required attention during selection as it will appreciably affect the end result.

Many researchers used these statistical techniques to find the relationships between processing parameters and clad geometry. Yuwen Sun et. al illustrated a statistical analysis technique to investigate the relation between clad geometry and input processing parameters. He concluded that an increase in powder feed rate and decrease in laser power had almost same effect by keeping other processing parameters same. Deposited thickness would increase if laser beam power or powder feed rate increase and scanning velocity decrease [52]. Yu-xin et.al analyzed statistically geometrical characteristics and properties of laser cladding, concluding that main influencing factor for layer height was mass flow rate and laser scan speed. On the other hand, laser scanning speed and laser power had more influence on layer width [53]. Eun Mi Lee et.al studied the effects of processing parameters on the single track of M4 powder by using DoE technique and concluded that size of bead increased as laser power increased because of the increment of melting more material. Bead height had most effect of increasing powder flow rate. Conversely bead width and dilution did not exhibit that big change of increasing powder flow rate [54]. Huaming Liu et. al investigated statistical relationship between processing parameters and clad geometry by using full factorial design taking laser power, scanning speed and powder thickness as processing parameters. An increment in powder thickness increased the clad size likewise laser power caused layer width to increase and scanning velocity had a negative effect on it [55]. Shuang Liu et al. statistically investigated the effect of input processing parameters on clad geometry, concluding that both laser power and mass flow rate effected clad width positively, powder feed rate and clad height but if the laser power increased up to some level it affected layer height negatively [56]. S. Saqib et al. investigated statistical results for an experimental study by using ANOVA and ANN approaches to study bead shape and process parameter relationship [57]. Manonmani et al. concluded that RSM is one of the major applications of DoE [58]. Davim investigated an experimental and statistical technique (ANOVA) to study the effect of processing parameters on clad geometry and hardness of coating. He observed that clad height showed an increment with the laser power and powder mass flow and decrement with scanning velocity. Depth of penetration was increased with laser power and powder mass flow rate. Clad width was increased with powder mass flow rate and hardness of coating HV increased with laser power [59]. Oliveira et al. presented an empirical relationship by theoretical and experimental study. The model predicted an important role for the velocity of powder particles, if velocity of the particles would increase more laser power would be required to melt the material. [60].

2.8 Analytical Modelling

Analytical models are basically mathematical models having a closed form solution. It can also be demonstrated as a mathematical analytic function that can describe a mathematical relation between input processing parameters and response variables [61]. Huang presented an analytical model to compute the laser power attenuation through powder stream by using some optics theories (Lambert-Beer theorem, Mie’s theory, and heat equilibrium). He concluded that with increasing powder flow rate, the laser intensities were reduced. Particle temperatures decreased vaguely with increase in powder flow rate, whereas peak values of laser intensity decreased with an increment of feeding angles [38]. Picasso proposed a model to predict the relationship between laser power attenuation and powder particle size explaining the attenuation term, concluded that attenuation factor inversely dependent on the size of particle, as particle size decreased, powder concentration and ultimately power attenuation increased [62]. Jichang Liu et al. modelled a relationship between powder concentration and power density. Beam attenuation increases as to the point where powder consolidation point starts [63]. Pinkerton presented an analytical model to calculate the laser attenuation and powder temperature distribution at every point below a coaxial nozzle, by validating it from experimental results, it was concluded that intensity of laser power was increased by increasing powder feed rate and decreasing the powder particle size [64]. Pinkerton and Li made a mathematical model of powder concentration by doing experimental validation of powder stream from a coaxial nozzle jet, it was found that the radius of powder stream had a negative impact on particle concentration at merging point. Powder stream radius depends on the size and morphology of the powder particles [65]. Fu et al. presented a mathematical equation by considering the effect of temperature and particle size, as the particle size increased the temperature distribution would decrease as more energy was absorbed by the powder particles [39]. Liu et al. analytically modelled laser beam attenuation during LMD process. It was concluded that attenuation increased with increase in powder feed rate and stand-off distance between nozzle and substrate [66]. Toyserkani et al. presented a mathematical model and concluded that it is impossible for deposition to occur if substrate is positioned before the convergence point of coaxial nozzle [67]. Neto presented an analytical model illustrating the influence of the distance between the origin of the divergent powder jet and the lens position on the temperature distribution in the particles that intercept the laser beam, and it was shown that this parameter had considerable influence on the energy use efficiency. The maximum temperature increased as distance decreased [68]. Haider et al. presented explicit equations for the terminal velocity and drag coefficient of falling spherical and non-spherical particles. To measure drag coefficient for non-spherical powder one needed a measure of particle shape and particle size, particle sphericity is used to measure the shape of particle [69]. Cheikh et al. presented an analytical relationships between the laser tracks and the processing parameters using 316L stainless steel powder, results showed that keeping laser power constant, layer track height and the cross section area decreased if the scan velocity increased and an increment had been observed if the powder flow rate increased, on the other hand, if powder flow rate and velocity remained constant, as laser power increased track area increased and so the more mass incorporated per meter (g/m) [70].

2.9 LMD Applications

Research have been carried out broadly in AM and concisely in LMD process and it indicated a wide range of applications. Main reason behind this research is the flexibility in different processing parameters that are difficult to machine and building end products having complex shapes. LMD does not cost the complexity of design. Some of applications has been found as below:

- Repair and production of components for aviation and aerospace industries [6]
- Tools reconfiguration/ Repair and restoring of tools [71]
- Cladding by LMD process [72]
- To increase the structural properties of parts for example hardness, fatigue and yield strengths [73]
- This process can be used where less heat effected zones are necessary [74]
- Building smart components
- Thermal Spraying and Electroplating [75]
- In medical, creation of surgical instruments and implants [76]

2.10 Summary

A detailed literature review has been discussed pertaining following subjects:

- AM Generic processes
- LMD process and subsystems
- LMD processing parameters and their effect on clad geometry
- Advancement in LMD modelling
- Dimensional Modelling
- Statistical Modelling
- Analytical Modelling
- LMD Applications

Chapter 3

DIMENSIONAL MODELLING

3.1 Introduction

Dimensional Analysis is a method, where physical quantities are exhibit in terms of their fundamental dimensions. In dimensional analysis, we predict the dependent and independent physical parameters that will affect the complete process, and then we group these processing parameters into dimensionless variables which enable a apprehend understanding of the process. Time [T], length [L], mass [M] and are three fundamental dimensions, but if the experiment involves heat then the temperature is another fixed dimension. These fixed dimensions are known as fundamental dimensions. The seven fundamental quantities are described in Table 3.1 below:

Table 3-1 Seven Fundamental Quantities [77]

Base Quantity	**Symbol for Dimension**
Length	L
Mass	M
Time	T
Electric Current	I
Temperature	Θ
Amount of Substance	N
Luminous Intensity	J

Apart from fixed dimensions some secondary quantities which own combination of fundamental dimensions. For example, velocity is denoted by distance covered per unit time (L/T), density can be described by mass per unit volume (M/L^3) and power as (ML^2T^{-3}). So these quantities become a secondary or derived quantity.

3.2 Methods of Dimensional Modelling

If the variables involved in a analysis are known, the dimensional relations between these variables is obtained by two methods [78]:

1. Rayleigh's Method
2. Buckingham's π-Theorem

3.2.1 Rayleigh's Method

This method is used for getting the expression for a variable which depends only on three or four variables. A functional relationship between dependent and independent variables can be expressed in an exponential relation, dimensionally homogeneous. A brief procedure of this method is given below [79]:

- Write a fundamental relationship of the data given
- Write an exponential equation of relation
- Selection of an appropriate system of fundamental dimensions
- Substitution of dimensional physical quantities
- Application of principle of dimensional homogeneity
- Equation of the exponents and their computation values
- Substitution of the exponent values
- Simplifying the given expression

3.2.2 Buckingham's π-theorem

A more generalized method of dimension analysis. Rayleigh's Method becomes difficult if the variables are more than the number of fundamental dimensions (M, L, T). To overcome this difficulty Buckingham's π-Theorem is a suitable option, which states, If there are "n" variables both dependent and independent in a physical phenomenon and if these variables contain "m" fundamental dimensions (M, L, T) then the variables are arranged into (n-m) dimensionless terms. Each term is called π term. This theorem is suitable where number of processing parameters are greater than four and it is not applicable if $(n-m) = 0$

3.3 Dimensional Evaluation

LMD is developed based on dimensional analysis. In LMD three sub process are considered including powder stream, melt pool and final geometry of the deposited layer as shown in Fig 3.1.

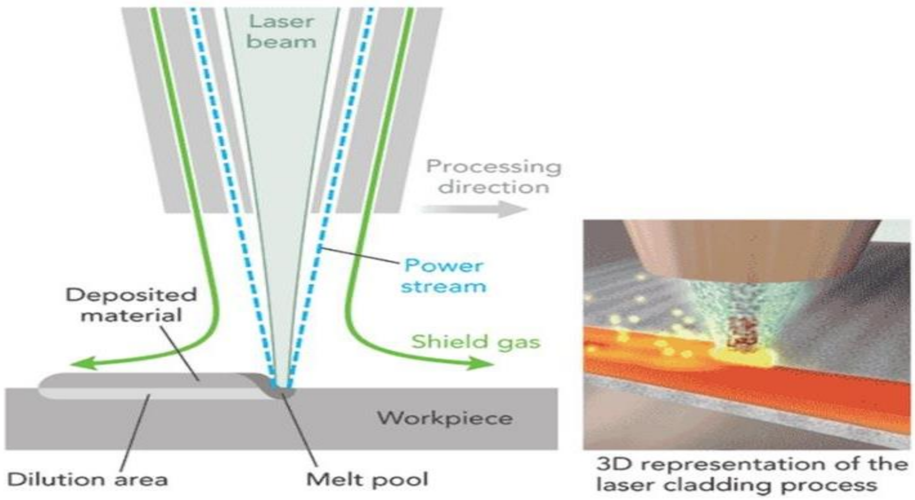

Figure 3-1 LMD Sub-Processes [80]

Considering powder stream as the main sub process, this process can further be divided into two groups of systems and are shown in Fig 3.2

- Material Delivery System
- Energy Delivery System

In dimensional analysis, three steps have been introduced to be performed by both material and energy delivery system. These three steps are the following:

Step 1: Listing of all independent and dependent variables in the form of dimensional matrix

Step 2: Calculation of the null matrix from the dimensional matrix

Step 3: Optimal arrangement of non-dimensional variables from the null basis

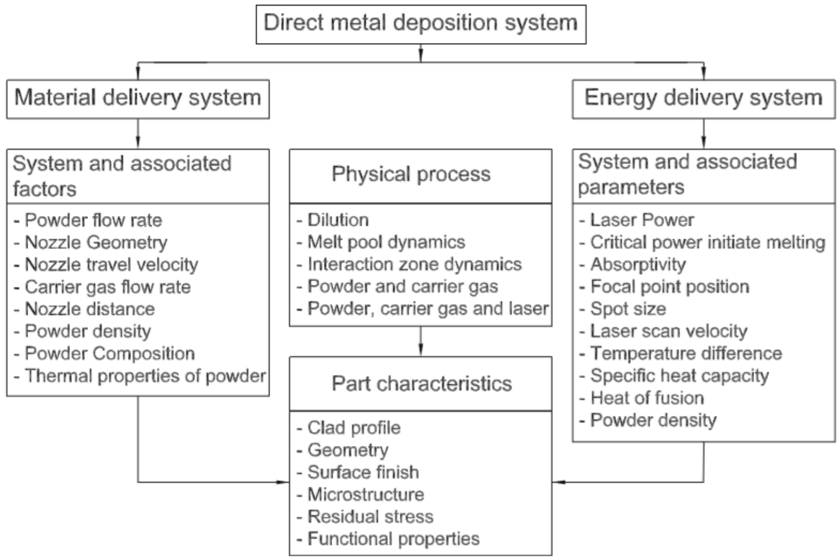

Figure 3-2 LMD Powder Stream Delivery Systems [13]

For modelling the process physically, the LMD process can be described as function of two systems,

- Energy Delivery System
- Material Delivery System

$$H_{LMD} = f(H_M, H_E) \tag{1}$$

Where H_M and H_E are the systems of the material delivery and energy delivery.

3.3.1 Material Delivery Model

The first groups of input parameters are related with material delivery model, which consists of following major factors as shown in Fig 3.3:

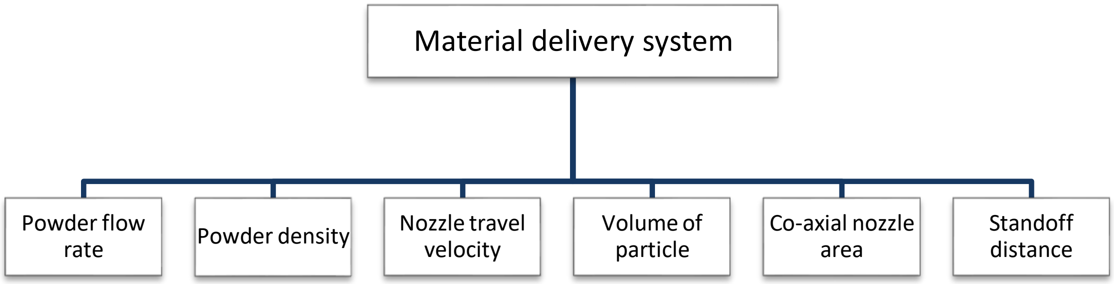

Figure 3-3 Major Factors Effecting Material Delivery System

Now by applying the three steps of dimensional modelling,

Step 1:

Layer height (H_M) is the dependent dimension and the independent variables influencing the layer height based on the material delivery system are powder size, powder flow rate, powder density, nozzle travel velocity, co-axial nozzle area, and nozzle standoff distance. In the material delivery system, it is assumed that powder supplied is efficiently deposited on substrate without any reflection. The major factors classified in terms of fundamentals units in Table 3.2. The dimensional matrix of the material delivery system is as follow:

$$D_1 = \begin{pmatrix} & H_m & \dot{m} & u & \rho & d & A_n & V_p \\ M & 0 & 1 & 0 & 1 & 0 & 0 & 0 \\ L & 1 & 0 & 1 & -3 & 1 & 2 & 3 \\ T & 0 & -1 & -1 & 0 & 0 & 0 & 0 \end{pmatrix} \tag{2}$$

Step 2:

The null basis of [D_1] results in four solution vectors which are as follow:

$$\begin{pmatrix} 2 & -1 & -2 & -3 \\ -1 & 0 & 0 & 0 \\ 1 & 0 & 0 & 0 \\ 1 & 0 & 0 & 0 \\ 0 & 1 & 0 & 0 \\ 0 & 0 & 1 & 0 \\ 0 & 0 & 0 & 1 \end{pmatrix}$$

Step 3:

There are four non-dimensional variables that are obtained from the solution vector as:

$$\pi_1 = H_m^2 \dot{m}^{-1} u\rho = \frac{H_m^2 u\rho}{\dot{m}} \tag{3}$$

$$\pi_2 = H_m^{-1} d \tag{4}$$

$$\pi_3 = H_m^{-2} A_n \tag{5}$$

$$\pi_4 = H_m^{-3} V_p \tag{6}$$

Functional relationship between these can be written as:

$$\pi_1 = f_1(\pi_2, \pi_3, \pi_4) \tag{7}$$

$$\frac{H_m^2 \rho u}{\dot{m}} = f_1\left(\frac{d}{H_m}, \frac{A_n}{H_m^2}, \frac{V_p}{H_m^3}\right) \tag{8}$$

$$H_m = C_1\left(\frac{\dot{m} d A_n V_p}{\rho u}\right)^{\frac{1}{8}} \tag{9}$$

3.3.2 Energy Delivery Model

The 2nd group is related with energy delivery and main input processing parameters as listed in Fig 3.4

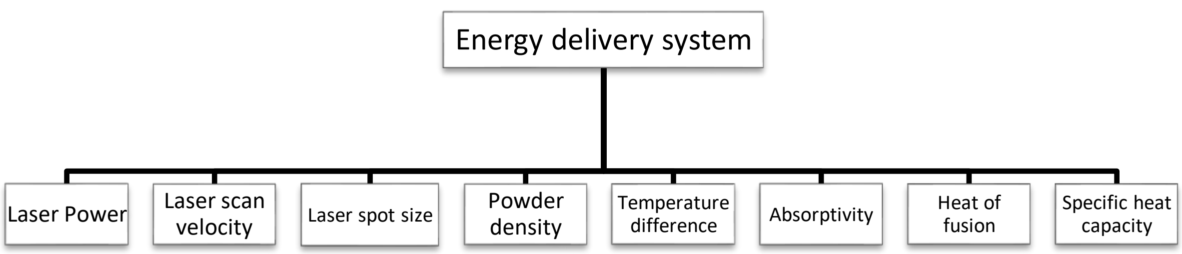

Figure 3-4 Major Factors Effecting Energy Delivery System

Step 1:

Layer height (H_E) is taken as dependent and major energy factors such as laser power, laser scan velocity, difference between melting temperatures, absorptivity, and temperature of substrate, heat of fusion, and specific heat as independent factors. The major factors classified in terms of fundamentals units in Table 3.2. The dimensional matrix of energy delivery system is as follows:

$$D_2 = \begin{array}{c} \\ M \\ L \\ T \\ t \end{array} \begin{pmatrix} H_E & u & P & s & \rho & T_m & C_p & h_f & \in \\ 0 & 0 & 1 & 0 & 1 & 0 & 0 & 0 & 0 \\ 1 & 1 & 2 & 1 & -3 & 0 & 2 & 2 & 0 \\ 0 & -1 & -3 & 0 & 0 & 0 & -2 & -2 & 0 \\ 0 & 0 & 0 & 0 & 0 & 1 & -1 & 0 & 0 \end{pmatrix} \tag{10}$$

Step 2:

The null basis of [D_2] results in four solution vectors which are as follow:

$$\begin{pmatrix} -1 & 2 & 0 & 0 & 0 \\ 0 & 3 & -2 & -2 & 0 \\ 0 & -1 & 0 & 0 & 0 \\ 1 & 0 & 0 & 0 & 0 \\ 0 & 1 & 0 & 0 & 0 \\ 0 & 0 & 1 & 0 & 0 \\ 0 & 0 & 1 & 0 & 0 \\ 0 & 0 & 0 & 1 & 0 \\ 0 & 0 & 0 & 0 & 1 \end{pmatrix}$$

Step 3:

The five non-dimensional variable that are obtained from above solution vector can be described as:

$$\pi_5 = H_E^{-1} s \tag{11}$$

$$\pi_6 = H_E^2 u^3 (P)^{-1} \rho = \frac{H_E^2 u^3 \rho}{(P)} \tag{12}$$

$$\pi_7 = u^{-2} \Delta T_m C_p = \frac{\Delta T_m C_p}{u^2} \tag{13}$$

$$\pi_8 = u^{-2} h_f = \frac{h_f}{u^2} \tag{14}$$

$$\pi_9 = \in \tag{15}$$

Functional relationship among all these non-dimensional variables can be written as:

$$\pi_5 = f_2(\pi_6, \pi_7, \pi_8, \pi_9) \tag{16}$$

$$H_E^{-1} s = f_2\left(\frac{H_E^2 u^3 \rho}{P}, \frac{\Delta T_{mC_p}}{u^2}, \frac{h_f}{u^2}, \in\right) \tag{17}$$

$$\mathbf{H_E} = \mathbf{C_2}\left(\frac{\mathbf{suP}}{\mathbf{\in h_f \Delta T_m C_{p\rho}}}\right)^{\mathbf{1/3}} \tag{18}$$

Table 3-2 Major Factors influencing the Layer Height of Clad Geometry

Parameters	Units
1. Material Delivery System	
Powder feed rate	m = $[MT^{-1}]$
Nozzle travel velocity	v = $[LT^{-1}]$
Material powder density	ƥ = $[ML^{-3}]$
Standoff distance	d = [L]
Co-axial nozzle area	$A_n = [L^2]$
Volume of particle	$V_p = [L^3]$
2. Energy delivery system	
Laser Power	$P=[ML^2T^{-3}]$
Laser scan velocity	$v=[LT^{-1}]$
Laser spot size	s=[L]
Material powder density	$\rho=[ML^{-3}]$
Temperature difference	$\Delta T_m=[t]$
Specific heat capacity	$C_p=[L^2T^{-2}t^{-1}]$
Heat of fusion	$h_f=[L^2T^{-2}]$
Absorptivity	ϵ = Dimensionless

Thus, layer height deposited in LMD cab be calculated by putting Eq.9 and Eq.18 into Eq.1

$$H_{LMD} = f\left[\left(C_1(\frac{\dot{m}dA_nV_p}{\rho u})^{1/8}\right), \left(C_2(\frac{suP}{\epsilon\ h_f\Delta T_mC_{p\rho}})^{1/3}\right)\right] \quad (19)$$

$$H_{LMD} = C(\frac{\dot{m}dA_nV_p}{\rho u})^{1/8}(\frac{suP}{\epsilon\ h_f\Delta T_mC_{p\rho}})^{1/3} \quad (20)$$

3.4 Value of C (Dimensionless Constant)

Regression analysis method has been used to get a relation to get the value of dimensionless constant that enables the predicted result to verify the experimental result. Dimensionless constant C consider both the experimental and theoretical results.

By using the above mathematical dimensional modelling method and putting values from an experimental work [81] as given in Table 3.3, predicted values of layer height can be calculated from Eq. 21, by finding the values of ‘C’ and ‘B’ as given in Eq. 22 and Eq.23.

$$Hp = CHLMD + B \quad (21)$$

$$C = \frac{n(\sum(Hth * \text{Hexp})) - (\sum Hth)(\sum \text{Hexp})}{n\sum(Hth)^2 - (\sum Hth)^2} \quad (22)$$

$$B = \overline{Hexp} - C\overline{Hth} \quad (23)$$

Table 3-3 Geometric and Material Parameters used in Calculations

1. Material Delivery System		**2. Energy Delivery System**	
Parameters	**Value**	**Parameters**	**Value**
Powder flow rate: m (g/s)	0.12, 0.18, 0.24 and 0.30	Laser Power: P (W)	800 and 1000
Nozzle travel velocity: u (mm/s)	4	Laser scan velocity: u (mm/s)	4
Powder density: ᵽ (g/mm^3)	0.008	Laser spot size: s (mm)	1.7
Standoff distance: d (mm)	7.5	Powder density: ᵽ (g/mm^3)	0.008
Co-axial nozzle area: A_n (mm^2)	33	Temperature difference: ΔT_m (C^o)	1630
Volume of particle: V_p (mm^3)	0.000261 (SP) and 0.002346 (LP)	Specific heat capacity: C_p ($J/g/C^o$)	0.477
		Heat of fusion: h_f (J/g)	260
		Absorptivity: ϵ (dimensionless)	0.11

The experiment has been done for two different laser powers and four different mass flow rates keeping the morphology of powder and powder size as a small fragment (SF) and large fragment (LF). Table (3.4 - 3.7) shows the experimental and predicted values of layer height at 800W and 1000W laser power keeping in mind the morphology and size of the particle as illustrated graphically in Fig (3.5-3.8).

Table 3-4 Small Fragment Layer Height Data

Small Fragment						
Laser Power (w)	**Mass Flow Rate (g/s)**	**HLMD (mm)**	**C**	**B**	**Hp (mm)**	**Hexp (mm)**
800	0.12	2.616	2.39	-5.46	0.7922	0.7
	0.18	2.752	2.39	-5.46	1.1172	1.094
	0.24	2.853	2.39	-5.46	1.3586	1.392
	0.3	2.933	2.39	-5.46	1.5487	1.558

Table 3-5 Small Particles with 1000w Power Layer Height Data

Small Fragment						
Laser Power (w)	**Mass Flow Rate(g/s)**	**HLMD (mm)**	**C**	**B**	**Hp (mm)**	**Hexp (mm)**
1000	0.12	2.818	4.25	-11	0.976	0.668
	0.18	2.964	4.25	-11	1.597	1.006
	0.24	3.073	4.25	-11	2.060	1.25
	0.3	3.16	4.25	-11	2.43	1.482

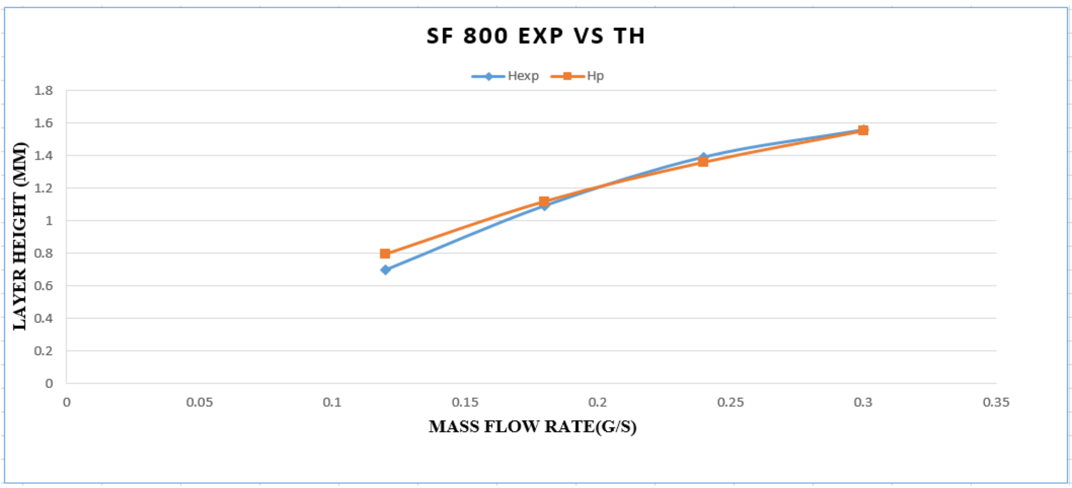

Figure 3-5 Graphical Representation of Hp vs Hexp (SF with laser power of 800w)

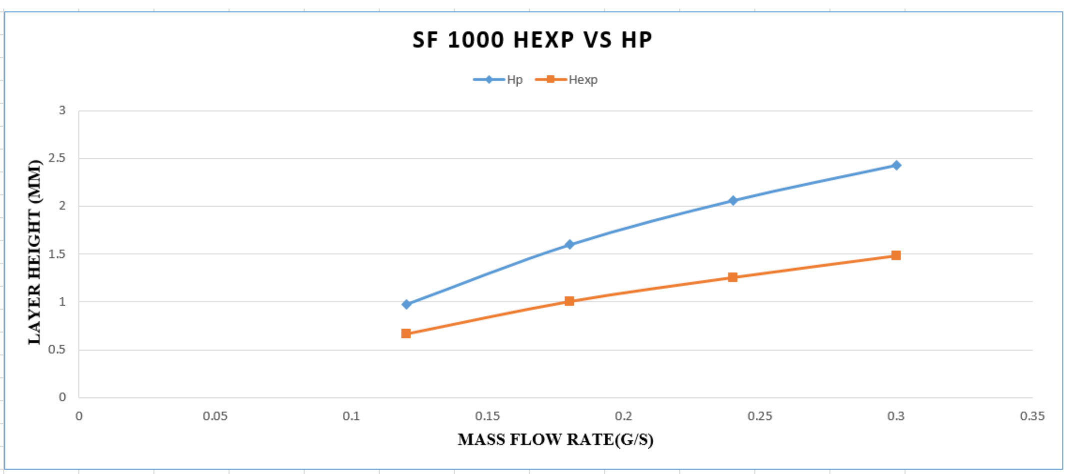

Figure 3-6 Graphical Representation of Hp vs Hexp (SF with laser power of 1000w)

Table 3-6 Large Fragment with 800kw Power Layer Height Data

Large Fragment						
Laser Power (w)	**Mass Flow Rate(g/s)**	**HLMD (mm)**	**C**	**B**	**Hp (mm)**	**Hexp (mm)**
800	0.12	3.442	1.625	5.28	0.313	0.384
	0.18	3.621	1.625	5.28	0.604	0.584
	0.24	3.754	1.625	5.28	0.820	0.772
	0.3	3.86	1.625	5.28	0.992	0.99

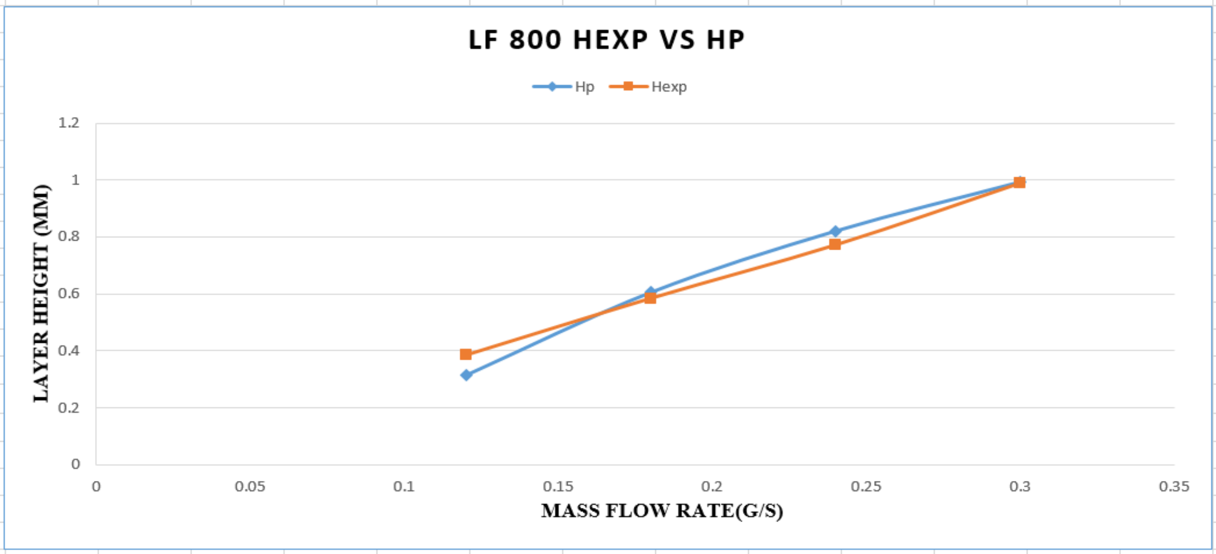

Figure 3-7 Graphical Representation of Hp vs Hexp (LF with laser power of 800w)

Table 3-7 Large Fragment with 1000w Power Layer Height Data

Large Fragment						
Laser Power (w)	**Mass Flow Rate(g/s)**	**HLMD (mm)**	**C**	**B**	**Hp (mm)**	**Hexp (mm)**
1000	0.12	3.7082	0.925	2.29	1.1400	0.42
	0.18	3.9009	0.925	2.29	1.3184	0.6
	0.24	4.0438	0.925	2.29	1.4505	0.718
	0.3	4.1582	0.925	2.29	1.5563	0.838

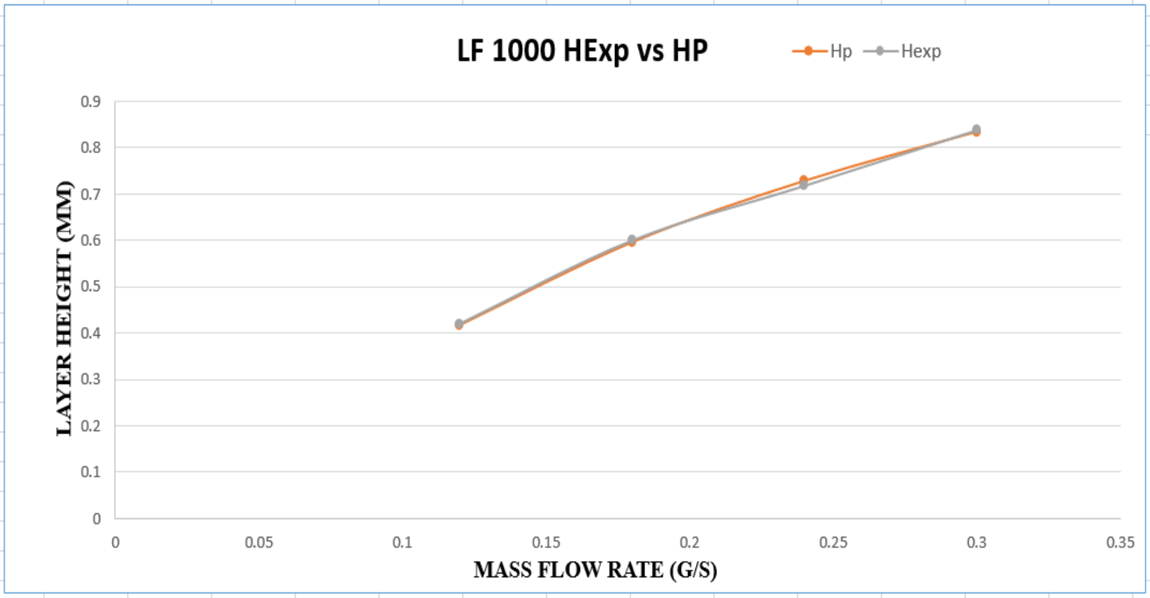

Figure 3-8 Graphical Representation of Hp vs Hexp (LF with laser power of 1000w)

3.5 Results & Discussions

Experimental results are in good agreement with predicted results when particle type is small. It has been observed that as laser power increases from 800W to1000W, layer height will also increase at some extent showing optimum results but after that, increased laser power will cause a reduction in layer height. As the laser power increases temperature increases and high temperature causes the liquid viscosity to decrease, consequently material can spread out [82]. Also if the morphology of particle changes from SF to LF, a change in layer deposition has been observed. As particle size increases the temperature distribution changes, LF will absorb more energy and it would effect melt pool as more energy would be required to melt the bigger particles and overall deposited height would decrease. Large particles attenuate the laser energy more and powder dispersion becomes more widespread as a result catchment efficiency decreases and fewer particles deposit that decrease the layer height. So, powder size and regularity has an impact on the deposited layer. As morphology of the particle deviates from the spherical size it will definitely affect the shape and size of deposited layer [59].

3.6 Summary

A dimensional mathematical model of the layer deposited using Π Backingum theorem has been formulated by considering main material processing parameters and main energy processing parameters that affect the layer height deposited by LMD techniques. After creating a relationship a dimensionless constant 'C' comes in the equation. The value of C is calculated using regression analysis technique. The properties of material are taken from an experimental work of material 316L steel. This model is validated for mass flow rate and laser power only; keeping scan velocity as constant parameter.

Chapter 4

STATISTICAL MODELLING

4.1 Introduction

Statistical modelling has been under consideration of many researchers since the advent of laser metal deposition process. The main reason of this method is to avoid physical phenomenon involved in the process [42]. Statistical modelling is an alternative to find the relationship between clad geometry and processing variables. For statistical studies data is typically obtained from some experiment or different kind of surveys.

4.2 Design of Experiments (DoE)

DoE is the branch of statistics which deals with analysis and design of experiments or surveys, widely in many domains especially marketing, medicine and engineering [83]. DoE helps to reduce experimental repeated effort. Experimental results usually predicted based on statistical methods and the responses of process parameters on experimental results can be deduced [70].

4.2.1 Statistical Terms and Concepts

Some statistical concepts that has been used in DoE are as follows:

4.2.1.1 Data

Some factors that can show variation during experiment can be categorized as process variables, such as the scanning speed of nozzle or mass flow rates and power of laser beam. Process variables can be split into continuous / numerical and categorical type.

Continuous data can be varied between a ranges, for example, a range of numbers as 23-34. Categorical data is restricted to a few distinct values for example small, medium and large.

4.2.1.2 Model

In analyzing an experiment, it is important to fit models relating response to the group of process control variables. Linear, factorial or quadratic model can be used as follows.

- Linear terms of the form $\alpha_i X_i$
- Two-factor interactions of the form $\alpha_{ij} X_i X_j$
- Quadratic terms of the form αX_i^2

4.2.1.3 Upper and Lower Limits of Data

For each numeric variable in data, it is required to fill upper and lower limits. The aim in defining limits is to make the range of variation.

4.2.1.4 Blocking

Mostly experiments are subjected to the means of contrast that are unneglectable but still can be forecasted in advance. For instance, if the experiment has to complete in many days of the week, possibly with some different humidity and ambient temperature. The design of experiments offered to split experiments into two or more blocks to rectify these unwanted sources of errors.

4.2.1.5 Randomization

Design of experiment automatically randomizes the data. Randomization reduces the possibility of unexpected sources of variation affecting the results and helps to meet the assumptions of the statistical methods that are used in analyzing experimental data.

4.2.1.6 Analysis of Data

Once experiment has been carried out, it is required to introduce the response values using different methods as RSM to study graphically the effects of process parameters on response variables.

4.2.1.7 Analysis of Variance (ANOVA) and Regression Analysis

Analysis of variance (ANOVA) is a collection of different statistical models that are used to predict and analyze the distinction between and among the groups [84]. ANOVA is one of the most widely used statistical methods for hypothesis testing. It can also be used as an alternative way of underlining which factors are active. Investigations that are analyzed by

ANOVA aim to assess the effect of various factors (mass flow rate, scan speed, laser power) on some response (layer width, layer height or hardness). ANOVA is a method that is used to compare the fit of two models; one model can be a modified version of the other model. The residuals are the differences between the given data and the predicted model. The exactness of the data with fitted model can be evaluated by sum of squared residuals. F-statistic is used in ANOVA table, F value is a tool to measure the variance between two population means that either they are significantly different or not. F value determines 'p' value that is the probability of getting a result. The p-value is normally evaluated from F-distribution table. If 'F' value is bigger than the critical 'F' values then the results are significant and in case of 'p' value if the 'p' values are smaller than the results are significant. P-values less than 0.05 are termed statistically significant, and those less than 0.01 are termed highly statistically significant.

Regression analysis is one of the most commonly used statistical technique to model the relationships between different variables, a part of the broader data analytic approach when it comes to solve the problem. Both linear and nonlinear regression can be done depending on the problem, it cover a wide range of applications including engineering, biological sciences, physics and chemistry [85]. In regression analysis, one variable is usually considered independent that can be used as a predictor variable (X) and the other dependent variable can be considered as an outcome of that predictor variable(Y). So by making linear or nonlinear equations having some data, this statistical approach can be used to broadly see the effect of variables [86].

4.2.1.8 Summary Statistics

One useful statistic here to measures the ratio between predicted response and estimated standard error that associate with the predictions.

4.2.1.9 Model graphs

DoE offers possibility to illustrate different plots to compare variation of response variables during the process.

4.3 Materials and Methods

4.3.1 Materials

Powder of different morphology has been taken of a solid block stainless steel of 316L under ambient condition. Table 4.1 gave the chemical composition of powder particles by Energy-dispersive X-ray spectroscopy (EDS) [81].

Table 4-1 Chemical Composition Measured through EDS

Element	Supplied Powder Particle (wt. %)	Powder Particles EDS (wt.%)
O	-	1.28
Mn	1.4	1.92
Si	0.53	0.44
Mo	2.1	2.4
Cr	16.8	17.61
Ni	10.4	10.29
Zr	-	-
Fe	68.77	65.79
C	-	0.27

The powder was classified using sieve method to produce batches of small and large fragments. Particle size <150mm was considered small fragment (SF) and sizes between 150–250mm was considered as large fragment (LF).

4.3.2 Methods

Thin walls were built by LMD from two different sizes of stainless steel 316L. A LDL160-1500 laser diode was used and material was fed by disc powder feeder [81].

4.3.2.1 DoE Technique

RSM is core applications of DoE, This technique has been used to predict the optimized results based on some mechanism of designed experiments [87]. FFD is the most common strategy of the experimental design containing many forms. This technique uses every possible combination of the factors values. In contrary to other design of experiment methods, this method does not distinguish anymore between disturbance and primary factors. Due to less number of observations, it is reasonable to use FFD in our modeling [88]. A series of experiments were designed and the results were analysed statistically, we applied three factors and two levels FFD based RSM. In the design particle type (A), laser power (B) and mass flow rates (C) were taken as main input factors and the aim was to identify their effect on clad geometry and their physical properties. Table 4.2 shows the upper and lower limits of process variables.

Table 4-2 Process Variables with Lower and Higher Limits

Process Variables	**Symbol**	**Low**	**High**
Particle type	A	SF	LF
Laser power(w)	B	800	1000
Mass flow rate(g/s)	C	0.12	0.3

The final model as coded factors is described in the equations (24-26)

$$Layer\ Height^{2} = 0.9439 - 0.4666 \times A - 0.0706 \times B + 0.6320 \times C + 0.0318 \times \mathrm{AB} - 0.2956 \times \mathrm{AC} - 0.0659 \times \mathrm{BC} \quad (24)$$

$$Layer\ width = 2.53 + 0.0163 \times A + 0.1200 \times B + 0.1470 \times C \quad (25)$$

$$Hardness = 190.53 - 10.90 \times A - 3.18 \times B + 2.55 \times C + 0.5969 \times AB - 4.45 \times AC + 1.15 \times BC \quad (26)$$

The equation in terms of actual factors can be used to make predictions about the response for given levels of each factor. Here, the levels should be specified in the original units for each factor as shown in (Equations 27-32):

Layer Height SF:

$$Layer\ height^{2} = -1.36021 + 0.000575B + 0.289641C - 0.000125B \times C \quad (27)$$

Layer Height LF:

$$Layer\ height^2 = -1.43055 + 0.001212B + 0.177030C - 0.000125B \times C \tag{28}$$

Layer Width SF:

$$Layer\ width\ = 1.08050 + 0.001200\ Laser\ Power + 0.028000\ Mass\ Flow\ Rate \tag{29}$$

Layer Width LF:

$$Layer\ width\ = 1.11300 + 0.001200\ Laser\ Power + 0.028000\ Mass\ Flow\ Rate \tag{30}$$

Hardness SF:

$$Hardness = 243.56080 - 0.065689B - 0.635357C + 0.002186\ B \times C \tag{31}$$

Hardness LF:

$$Hardness = 232.62248 - 0.053752B - 2.32921\ C + 0.002186\ B \times C \tag{32}$$

These set of equation can be used to predict the response variables for levels that are defined during analysis.

4.4 Results and Discussions

4.4.1 Statistical Analysis

Total 16 runs were executed during experimental study. The actual data was used to form the predicted data for three response variables to study empirically. Table 4.3 shows the obtained results.

Table 4-3 Predicted vs Actual Result Table of Two Level and Three Input Factor FFD

Run	Input Variables			Response Variables (Actual Vs Predicted)					
	A	B	C	Layer Height T'actual (mm)	Layer Height T'predicted (mm)	Layer Width W'actual (mm)	Layer Width W'predicted (mm)	Hardness actual HV0.3	Hardness predicted HV0.3
1	SF	800	11.0	1.094	1.04	2.29	2.35	202.43	203.26
2	SF	800	18.0	1.558	1.63	2.65	2.54	210.7	211.06
3	LF	800	11.0	0.584	0.5879	2.35	2.38	188.6	183.24
4	LF	1000	18.0	0.838	0.8668	2.75	2.82	176.5	176.30
5	SF	1000	18.0	1.482	1.49	2.74	2.78	204.89	205.79
6	LF	1000	7.5	0.42	0.4212	2.56	2.52	176.1	177.80
7	LF	800	7.5	0.384	0.3986	2.29	2.28	182.3	185.27
8	LF	1000	11.0	0.6	0.5697	2.63	2.62	180.5	177.30
9	SF	800	7.5	0.668	0.7162	2.53	2.49	189.52	189.50
10	LF	1000	14.5	0.718	0.7183	2.72	2.72	175.1	176.80
11	LF	1000	14.5	0.772	0.7771	2.44	2.48	179.8	181.21
12	SF	1000	11.0	1.006	0.9741	2.58	2.59	194.4	194.93
13	SF	800	7.5	0.7	0.7382	2.25	2.25	199.4	199.36
14	LF	800	18.0	0.99	0.9664	2.66	2.58	178.2	179.18
15	SF	1000	14.5	1.256	1.23	2.72	2.69	210.78	200.36
16	SF	800	14.5	1.392	1.34	2.38	2.45	208.31	207.16

The significant test was performed using Design Expert version 11 software to develop the model to describe the effects of response variables. The developed relationships were tested using a technique called ANOVA at the confidence interval of 98% as shown in Table (4.4-4.6). F statistics and p values has been used to determine either the model is significant or not, as F values were high and $p<0.05$. The values of 0.9966, 0.9161 and 0.9740 indicate the high correlation between the experimental and measured data. Adjusted R^2 and predicted R^2 are in good agreement and within range so as adequate precision values.

Table 4-4 Analysis of Variance for Layer Height (ANOVA)

Source	Sum of Squares	df	Mean Square	F-value	P-value	
Model	2.01	6	0.3351	148.92	<0.0001	Significant
A-particle type	0.9264	1	0.9264	411.69	<0.0001	
B-Laser power	0.0148	1	0.0148	6.56	0.0306	
C-Mass flow rate	0.9995	1	0.9995	444.17	<0.0001	
AB	0.0020	1	0.0020	0.8800	0.3727	
AC	0.0597	1	0.0597	26.55	0.0006	
BC	0.0083	1	0.0083	3.68	0.0873	
Residual	0.0203	9	0.0023			
Cor total	2.03	15				

R^2 = 0.9966
Adjusted R^2 = 0.9943
Predicted R^2 = 0.9870
Adequate Precision = 65.8274

Table 4-5 Analysis of Variance for Layer Width

Source	Sum of Squares	df	Mean Square	F-value	P-value	
Model	0.4267	3	0.1422	43.69	<0.0001	Significant
A-particle type	0.0042	1	0.0042	1.30	0.2769	
B-Laser power	0.2304	1	0.2304	70.77	<0.0001	
C-Mass flow rate	0.1921	1	0.1921	59.00	<0.0001	
Residual	0.0391	12	0.0033			
Cor total	0.4658	15				

R^2 = 0.9161
Adjusted R^2 = 0.8951
Predicted R^2 = 0.8407
Adequate Precision = 19.8563

Table 4-6 Analysis of Variance for Hardness

Source	Sum of Squares	df	Mean Square	F-value	P-value	
Model	2312.5	6	385.43	56.12	<0.0001	Significant
A-particle type	1899.43	1	1899.43	276.58	<0.0001	
B-Laser power	162.24	1	162.24	23.62	0.0009	
C-Mass flow rate	57.7	1	57.75	0.8300	0.0176	
AB	5.70	1	5.70	0.8300	0.3860	
AC	175.74	1	175.74	25.59	0.0007	
BC	11.71	1	11.71	1.71	0.2240	
Residual	61.81	9	6.87			
Cor total	2374.38	15				

R^2 = 0.9740
Adjusted R^2 = 0.9566
Predicted R^2 = 0.9263
Adequate Precision = 20.0515

In Fig 4.1 a comparison has been shown between actual and predicted values of response variables (layer height, width and hardness) by considering the input variables of particle type, laser power and mass flow rates. Predicted vales are in agreement with actual values with acceptable range of errors.

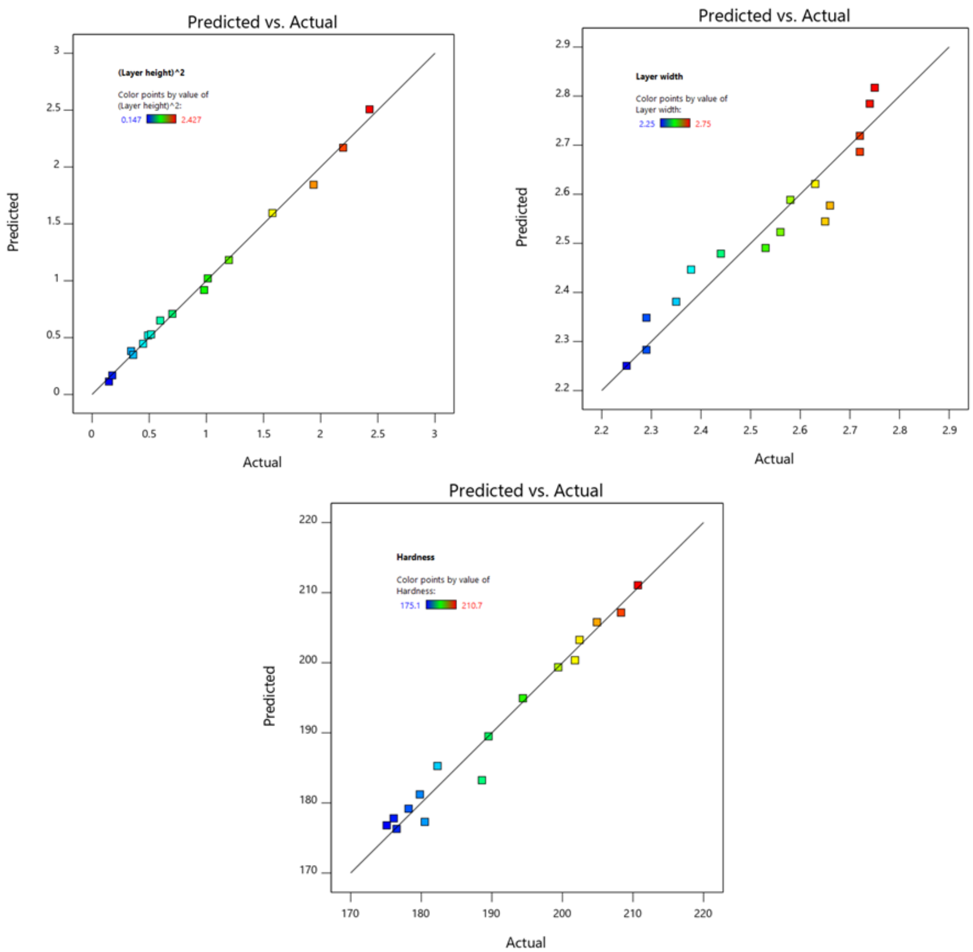

Figure 4-1Relationship b/w Predicted vs Actual Values: Layer Height, Layer Width and Hardness

.

4.5 Effect of processing parameters on clad geometry

The effects of input processing parameters on clad geometry (clad height, clad width, and hardness) were evaluated by perturbation and 3D surface plots.

4.5.1 Layer Height

In Fig 4.2 and Fig 4.3 perturbation and 3D surface plots have been shown to illustrate the effect of powder size, powder morphology and processing variables on layer height. It can be seen that the layer height has a positive effect of powder flow rate [53] [54]. As mass flow will increase it will cause more particles to deposit causing an increase in clad height.

It has been observed that as laser power increases upto the center point of design space, the layer height will increase and after the center point, a decrement in layer height has been observed. High temperature causes the liquid viscosity to decrease as a result material can spread out [56]. Large powder flow rate with medium laser power can produce large clad layer height.

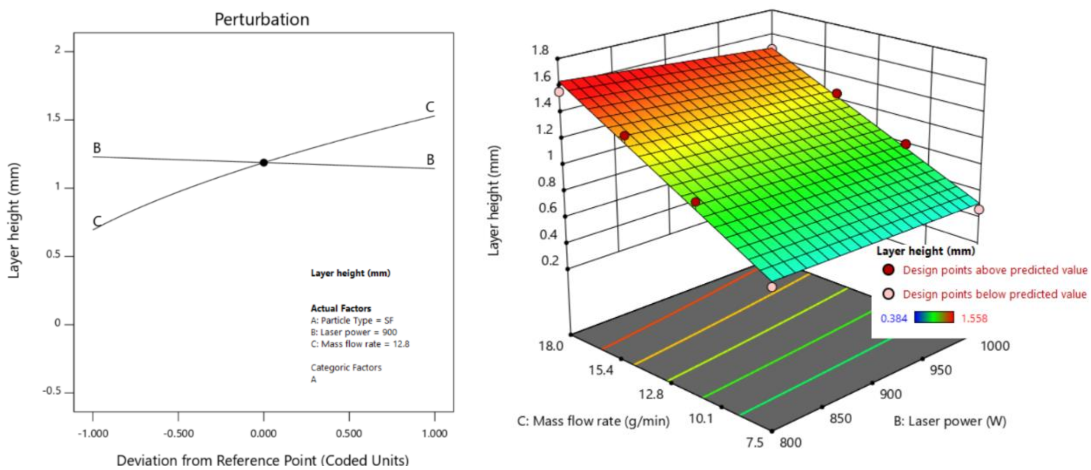

Figure 4-2 Perturbation Plot & 3D Surface Plot Influence of the Processing Parameters with SF on Clad Height

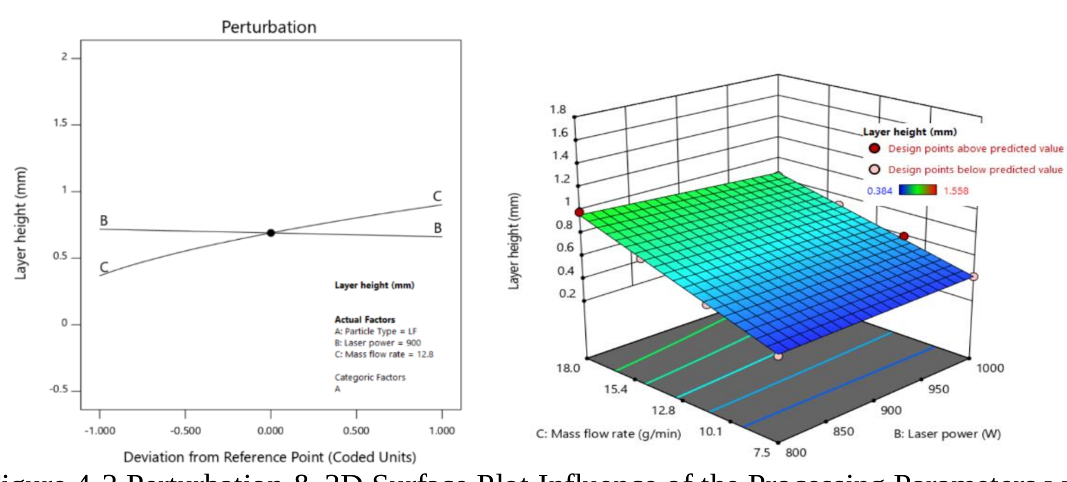

Figure 4-3 Perturbation & 3D Surface Plot Influence of the Processing Parameters with LF on Clad Height

Keeping in mind the particle morphology, it has been observed from perturbation & 3D surface plots (Fig 4.2 and Fig 4.3) as non-spherical powder morphology changes sizes from SF to LF it has a negative effect on layer height. The graphs have been shifted downward with the same trend. As the size of particle increases dispersion behavior of powder increases and more power is required to heat large shape particle that can also affect the molten pool qualities [49]. In the ANOVA Table 4.4, it can be seen that the interactive terms of both laser power and powder feeding rates are significant.

4.5.2 Layer Width

In Fig 4.4 and Fig 4.5 perturbation & 3D surface plots have been shown which illustrate the effects of powder morphology, powder size, and processing parameters.

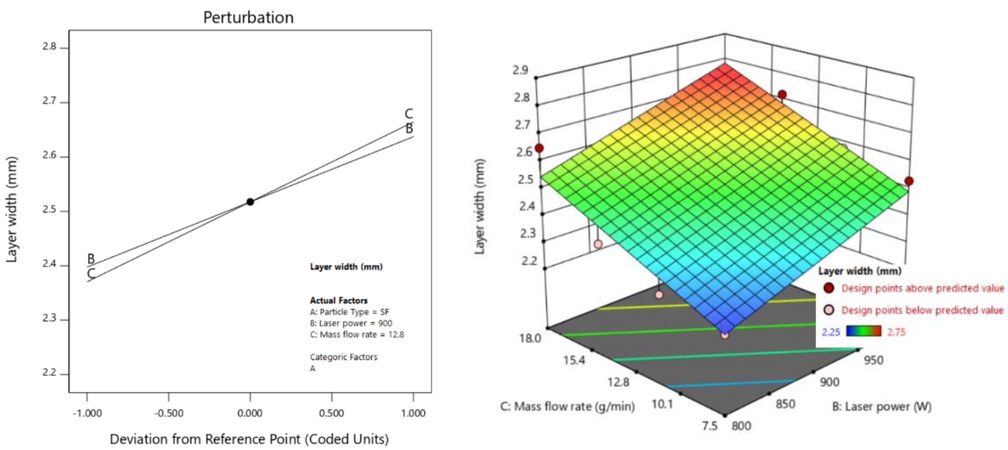

Figure **4-**4 Perturbation & 3D Surface Plot Influence of the Processing Parameters with SF on Clad Width

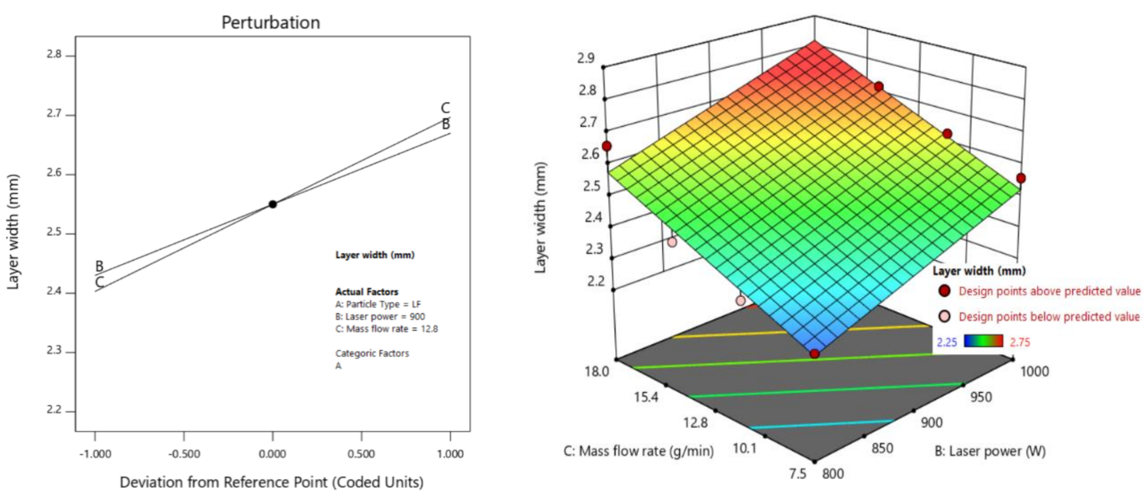

Figure 4-5 Perturbation & 3D Surface Plot Influence of the Processing Parameters with LF on Clad Width

It can be seen from graphs that both powder flow rate and laser power has a positive effect on layer width. As more powder flow rate would deposit more material and an increment in laser power will produce greater molten pool, consequently width will increase [53].

As non-spherical particle sizes increase layer width will increase. The graphs have been shifted upward with the same trend. In the ANOVA Table 4.5, it can be seen that the interactive terms of both laser power and powder feeding rates were significant.

4.5.3 Hardness

In Fig 4.6 and Fig 4.7 perturbation plot has been shown the effect of powder morphology and processing parameters on hardness.It can be seen that powder flow rate has increased the value of hardness, on the other hand on increasing laser power a negative trend in hardness has been observed.

By keeping in mind the morphology of powder, a linear increase in hardness has been observed as mass flow rate increases with small fragments but as particle fragment size increaseins it will cause temperature distribution disturbance that will reduce hardness.

In ANOVA Table 4.6, it can be seen that the interactive terms of both laser power and powder feeding rates are significant.

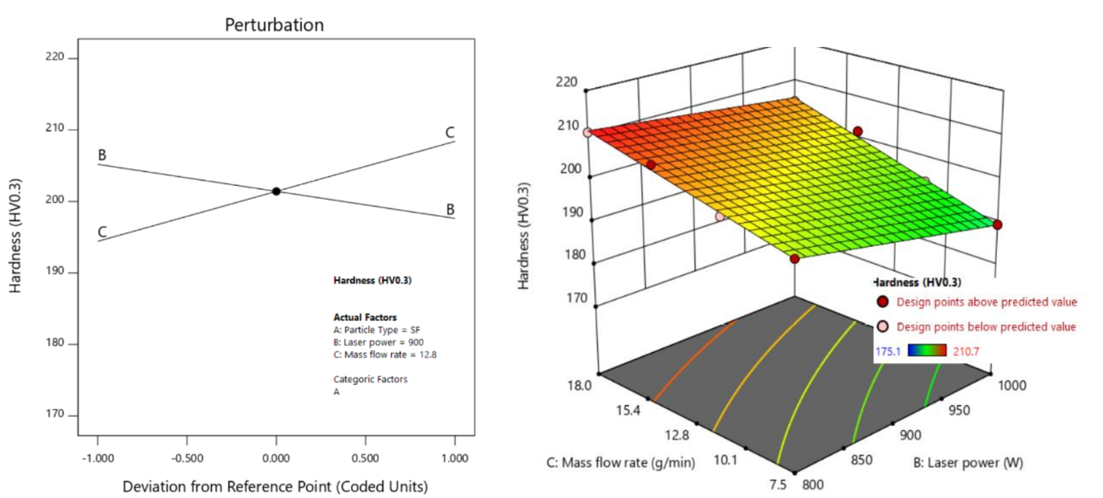

Figure 4-6 Perturbation & 3D Surface Plot Influence of the Processing Parameters with SF on Hardness

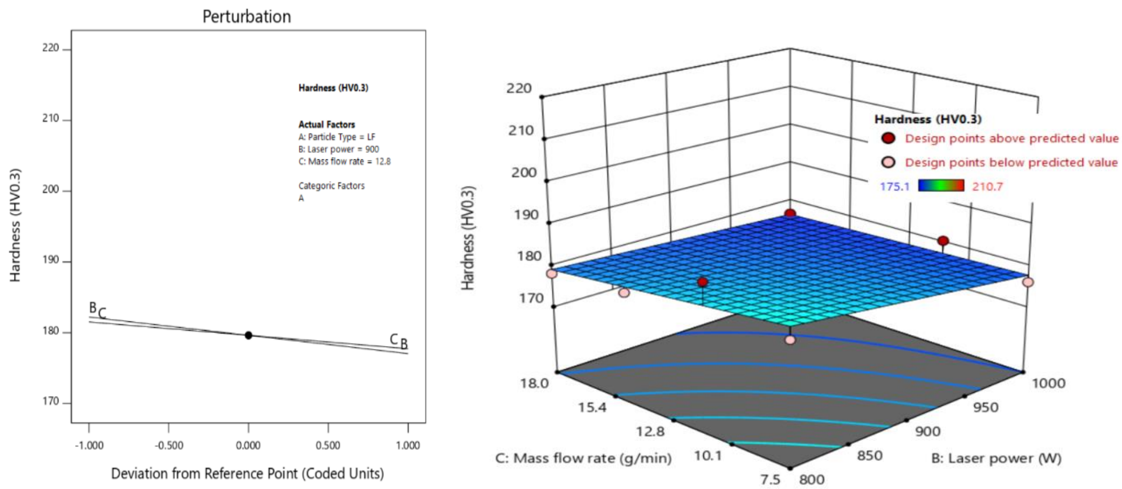

Figure 4-7 Perturbation & 3D Surface Plot Influence of the Processing Parameters with LF on Hardness

4.6 Summary

316L stainless steel was laser clad to study the effects of processing parameters on the clad dimension and hardness of the clad surface. Based on statistical analysis following conclusion were concluded.

- Results indicated that powder feed rate and powder morphology effected the layer height significantly. It was observed from perturbation plot that laser power effected layer height positively before reaching the central point of the design space, after that increment in laser power effected the layer height negatively. The reason behind that negative effect was change in viscosity that can cause the material to spread out. So, layer height showed a decrement with increment of laser power. Layer height decreased as the particle type changed from SF to LF.
- Layer width increased with the laser power; greater laser power brought more energy onto the substrate and thus resulted in wider melt pool. However, powder feed rate and powder type affected layer width positively.
- Mass flow rate effected hardness in a positive manner while particle type and laser power effected layer height negatively.

Chapter 5

ANALYTICAL MODELLING

5.1 Introduction

Analytical models are closed form mathematical models, i.e. a system of equations used to illustrate the variation in a system through a mathematical analytic function.

5.2 Effect of particle properties

Particle properties are an important parameter in LMD processes and it affects many other sub processes of LMD. The properties of metallic powder can be described in fig 5.1.

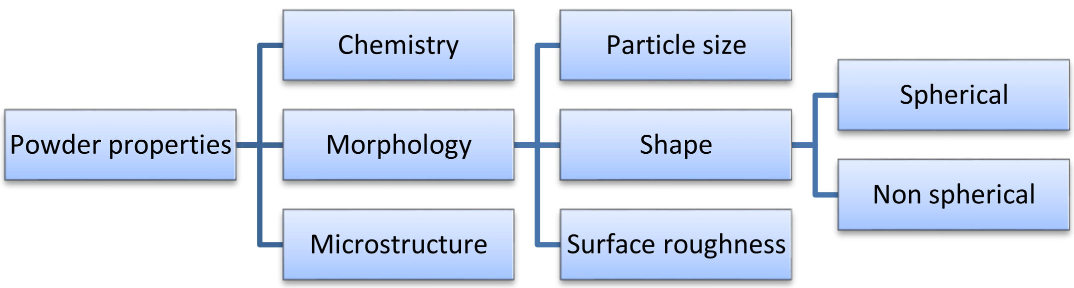

Figure 5-1Powder Properties

Powder properties can be classified as chemical, morphology and microstructure. In our thesis we will focus on powder morphology. Powder morphology effects following parameters LMD:

- Power Attenuation
- Concentration of Particles in Powder Stream
- Temperature Distribution

5.2.1 Review of Analytical Modelling

During LMD when laser beam transmitted by the powder stream, it affected by many processing parameters.

1. Huang presented an analytical model to compute the laser power attenuation power through powder stream based on optics theories (Lambert-Beer theorem, Mie's theory, and heat equilibrium) [38]. A mathematical relationship can be seen from Eq.33

$$\mathrm{I(x,y,z) = I(x,y,z+\Delta z)\{1-\exp[\Pi Rp^2 N(x,y,z)Q\Delta z]\}} \qquad (33)$$

Where, I(x, y, z) is the laser intensity and I(x, y, z+Δz) is the incident laser intensity, Rp is the particle radius and N is the concentration of powder particles Q is extinction coefficient which takes into account wavelength of light. Here clearly the laser intensity will decrease with powder concentration. So as the powder concentration will increase the intensity of incident light would also decrease. Attenuation will cause energy and power degradation.

2. Picasso [62] proposed an analytical model to predict a relationship between laser power attenuation and powder particle size explaining the attenuation term as:

$$\boldsymbol{\beta} = \frac{\dot{\mathbf{m}}}{\mathbf{2\rho r_{jet}\ r_{p}\, v_{p}\ \ Cos\theta_{jet}}} \qquad (34)$$

Here from the above equation, it was concluded that attenuation factor inversely dependent on the size of the particle, as particle size decreased, it increased powder concentration and ultimately power attenuation would increase.

3. Liu et al. modelled a relationship between powder concentration and power density as [63]:

$$\begin{aligned} I(x,y) &= I_o\,(x,y)[1-\alpha n(x,y)] \\ &= 2AP\Pi r^2{}_b exp - 2(x^2+y^2)r^2{}_b 1 \\ &- \alpha 2n_p \Pi r^2{}_b \end{aligned} \qquad (35)$$

In above eq. $I(x, y)$ is power density at point (x, y) r_b is the value of radius where the laser beam narrowed from the intense value, n_p is the powder concentration. In the above relationship, it has been found that the power density of the laser beam decreases as powder concentration increases which affect the final product characteristics. Beam attenuation increases as to the point where the powder consolidation point starts.

4. Pinkerton presented an analytical method to calculate the laser attenuation and powder temperature distribution at each and every point below a coaxial nozzle, by validation it from experimental results, beam attenuation increased at the point below beam consolidation where coaxial beam converted into a single stream [64]. Powder particles when injected through nozzle followed different trajectories due to different sizes, and experienced different temperature depending on the range of distance they were keeping in laser beam as described in eq. below:

$$\frac{\partial \mathbf{I}}{\partial \mathbf{z}} \propto \frac{\dot{\mathbf{m}}}{\mathbf{r_p}} \tag{36}$$

Where intensity of laser power was increased by increasing powder feed rate and decreasing the powder particles.

5. Hung et al. [38] studied the effect of powder size concluding that as the particle size would increase; powder concentration in powder stream would decrease as shown in the eq. below:

$$N(x, y, z) = \frac{m}{\rho \frac{4\Pi Rp2vp}{3}} \cdot \frac{1}{\Pi R(x, y, z)2} \exp[\frac{r(x, y, z)2}{R(x, y, z)2}] \tag{37}$$

Where m is mass flow rate, is the density of particle, vp is particle speed.

6. Pinkerton and Li [65] made a mathematical model of powder concentration by doing experimental validation of powder stream from a coaxial nozzle jet, considering the whole process in two parts

- Before merging of powder stream in a coaxial nozzle
- After merging of powder stream in a coaxial nozzle

The mathematical expression is:

$$C(x,y) = \frac{4m}{Q\sqrt{\pi}} exp - \left[\frac{2Y}{(ro - ri)}\right]^2 \quad (38)$$

C(x, y) is the concentration of powder particles after merging of powder stream, the radius of powder stream $(ro - ri)$ had a negative impact on particle concentration at merging point. In this paper particles size from 53-150µm has been considered. Powder morphology has been considered as spherical. By considering particle shape as non-spherical, a mathematical model can be designed.

7. Fu et al. [39] presented a mathematical equation by considering the effect of temperature when the particle size was variable in some range as described below:

$$\mathrm{Q = \alpha p \Pi R p^2 l p} \quad (39)$$

Where Q is total energy absorbed by the particles of powder, αp is absorptivity of the particle, lp is an integer which depend on the trajectory of the particles. When the powder particles passed through the laser beam, they absorbed photons of energy and their temperature increased, if each particle had different size then particles would reach the substrate with different temperature and it would effect surely the melt pool and final characteristics of the part. As the particle size increased the temperature distribution would decrease as more energy would be absorbed by the powder particles, also temperature distribution has also been described from the eq. below:

$$\mathbf{T_p = T_0 + \frac{3\alpha_p l_p}{4 r_p \rho_p c}} \quad (40)$$

Where $\mathrm{l_p, r_p, \rho_p}$ *and c* were the latent heat per unit mass, radius of the particle, particle density and specific heat per unit mass respectively. As particle size increased, the temperature distribution of particles decreased.

5.3 Methods of Calculating Particle Size of Non-Spherical Particles

In LMD powder particles usually deviate from its spherical shape, it is ideal to get the spherical shaped powder particles, as during their making, some particles deviate from their spherical shape. So, it is important to know how to calculate the powder particle size which deviates from the spherical shape [89].

5.3.1 Equivalent Diameters

When it comes to non-spherical particles it is necessary to calculate equivalent diameters. Some important equivalent diameters are listed below:

5.3.1.1 Volume Equivalent Diameter

When the volume of the particle is given then it is very easy to find the equivalent diameter of particle:

$$D_{equivalent} = [\frac{6}{\Pi} V_{particle}]^\wedge \frac{1}{3} \tag{41}$$

Where D $_{equivalent}$ is the diameter of sphere with the same volume of the non-spherical particle.

5.3.1.2 Projected Area Diameter

Another method to calculate non-spherical particles diameter, it is the equivalent diameter of a sphere having same projected area. It is basically orientation dependent and can be measured by microscopic image analysis.

5.3.1.3 Equivalent Surface Diameters

Equivalent surface diameters are actually the diameters of spheres with the same surface as of particle and given by formula below:

$$D_{equivalent} = [\frac{6}{\Pi} S_{particle}]^\wedge \frac{1}{2} \tag{42}$$

5.4 Summary

In the chapter, analytical approaches were discussed to find the effect of particle morphology during the LMD process. We concluded the following results:

- Particle size has an inverse relation on power attenuation of the laser beam, as the size decreases attenuation will increase and due to increase in powder concentration intensity of incident laser power decreases.
- Particle size has an inverse relation with the temperature distribution of powder stream, as particle size increases temperature distribution will decrease as bigger particles will absorb more energy.
- Particle concentration has a negative impact on laser beam attenuation, as powder concentration will increase more attenuation will occur.
- As Particle size decreases, there will be more powder concentration in powder stream
- Different methods of calculating non-spherical diameter were also discussed.

Chapter 6

CONCLUSIONS AND FUTURE SUGGESTIONS

6.1 Conclusion

In this thesis, we have focused on the investigation of the effect of processing variables on the geometric features. We have investigated the effect of powder morphology in sub process of LMD. Powder stream is the main focus of study and different parameters that can affect the clad height, width and surface hardness are under consideration.

Dimensional modelling is done by using Bakingum Π-method and a relationship is made between layer height and major energy and material processing parameters. Material properties and processing parameters are taken from experimental data. Mass flow rate, laser power and particle size, and morphology have been taken as variable. A validation from an existing experimental work has been done.

Statistical modelling is done by using Design Expert software. By using statistical technique ANOVA, the effect of processing parameters on response surface has been investigated. Results shows that mass flow rates effect the layer height most as compare to laser power. Laser width shows a positive effect of increasing laser power and powder size as compared to mass flow rate. Surface hardness increases with increment in mass flow and decreases with decrement in laser power and non-spherical particle size.

In the last chapter, A review of the analytical modelling is done by keeping powder morphology and powder size in mind. It is found that particle morphology is an important parameter while studying powder stream and it affects the whole process. When a particle deviates from its spherical shape it affects powder stream in sense of temperature distribution, particle concentration, and energy attenuation. As particle size increases or deviates from spherical shape, powder concentration and temperature distribution decreases, as bigger and irregular particles will absorb more temperature and concentration will also decrease due to low packing factor.

6.2 Future Recommendations

For further study powder morphology and its effect on clad height and width, analytical modelling is needed so that a clear mathematical equation could help researchers to study how the shape of the particle will affect the final clad geometry. An optimized study will be helpful to know how non-spherical shape will affect laser beam and the temperature distribution as in literature powder shape is mostly considered spherical.

This work thus can be extended to detailed analytical modelling process by adding particle morphology in it.

REFERENCES

1. Ian Gibson, David Rosen, Brent Stucker. Additive Manufacturing Technologies, 3D Printing, Rapid Prototyping, and Direct Digital Manufacturing, Second Edition ISBN: 978-1-4939-2112-6
2. Santos, E.C., Shiomi, M., Osakada, K. and Laoui, T., 2006. Rapid manufacturing of metal components by laser forming. International Journal of Machine Tools and Manufacture, 46(12-13), pp.1459-1468.
3. Kumar, A., Paul, C.P., Pathak, A.K., Bhargava, P. and Kukreja, L.M., 2012. A finer modeling approach for numerically predicting single track geometry in two dimensions during Laser Rapid Manufacturing. Optics & Laser Technology, 44(3), pp.555-565.
4. Pinkerton, A.J., Wang, W. and Li, L., 2008. Component repair using laser direct metal deposition. Proceedings of the Institution of Mechanical Engineers, Part B: Journal of Engineering Manufacture, 222(7), pp.827-836.
5. Selcuk, C., 2013. Joining processes for powder metallurgy parts. In Advances in Powder Metallurgy (pp. 380-398). Woodhead Publishing.
6. Graf, B., Ammer, S., Gumenyuk, A. and Rethmeier, M., 2013. Design of experiments for laser metal deposition in maintenance, repair and overhaul applications. Procedia CIRP, 11, pp.245-248.
7. Rylands, B., Böhme, T., Gorkin III, R., Fan, J. and Birtchnell, T., 2016. The adoption process and impact of additive manufacturing on manufacturing systems. Journal of Manufacturing Technology Management, 27(7), pp.969-989.
8. Javaid, M. and Haleem, A., 2019. Current status and challenges of Additive manufacturing in orthopaedics: an overview. Journal of clinical orthopaedics and trauma, 10(2), pp.380-386.
9. Settling the Debate: CNC Machining VS. 3D Printing. http://buntyllc.com/settling-the-debate-cnc-machining-vs-3d-printing/. Accessed 2 Nov 2017
10. Shahzad, K., Deckers, J., Kruth, J.P. and Vleugels, J., 2013. Additive manufacturing of alumina parts by indirect selective laser sintering and post processing. Journal of Materials Processing Technology, 213(9), pp.1484-1494.
11. Ramakrishnan, A. and Dinda, G.P., 2019. Direct laser metal deposition of Inconel 738. Materials Science and Engineering: A, 740, pp.1-13.
12. Sun, G.F., Shen, X.T., Wang, Z.D., Zhan, M.J., Yao, S., Zhou, R. and Ni, Z.H., 2019. Laser metal deposition as repair technology for 316L stainless steel: Influence of feeding powder compositions on microstructure and mechanical properties. Optics & Laser Technology, 109, pp.71-83.
13. Spears, T.G. and Gold, S.A., 2016. In-process sensing in selective laser melting (SLM) additive manufacturing. Integrating Materials and Manufacturing Innovation, 5(1), p.2.

14. Wirth, F., Arpagaus, S. and Wegener, K., 2018. Analysis of melt pool dynamics in laser cladding and direct metal deposition by automated high-speed camera image evaluation. Additive Manufacturing, 21, pp.369-382.
15. McNutt, P.A., 2015. An investigation of cracking in laser metal deposited nickel superalloy CM247LC (Doctoral dissertation, University of Birmingham).
16. Allmen, M.V. and Blatter, A., 2013. Laser-beam interactions with materials: physical principles and applications (Vol. 2). Springer Science & Business Media.
17. Mahamood, R.M., Akinlabi, E.T., Shukla, M. and Pityana, S., 2014. Characterization of laser deposited Ti6Al4V/TiC composite powders on a Ti6Al4V substrate.
18. Thayalan, V. and Landers, R.G., 2006. Regulation of powder mass flow rate in gravity-fed powder feeder systems. Journal of manufacturing processes, 8(2), pp.121-132.
19. Rein, G. and Andrés, A., 2001. Computer simulation of granular material: vibrating feeders. Powder Handling & Processing, 13(2), pp.181-185.
20. Pan, H., Landers, R.G. and Liou, F., 2006. Dynamic modeling of powder delivery systems in gravity-fed powder feeders. Journal of manufacturing science and engineering, 128(1), pp.337-345.
21. Gu, D.D., Meiners, W., Wissenbach, K. and Poprawe, R., 2012. Laser additive manufacturing of metallic components: materials, processes and mechanisms. International materials reviews, 57(3), pp.133-164.
22. Liou, F., Slattery, K., Kinsella, M., Newkirk, J., Chou, H.N. and Landers, R., 2007. Applications of a hybrid manufacturing process for fabrication of metallic structures. Rapid Prototyping Journal, 13(4), pp.236-244.
23. Huang, Y., Khamesee, M.B. and Toyserkani, E., 2016. A comprehensive analytical model for laser powder-fed additive manufacturing. Additive Manufacturing, 12, pp.90-99.
24. Brandl, E., Schoberth, A. and Leyens, C., 2012. Morphology, microstructure, and hardness of titanium (Ti-6Al-4V) blocks deposited by wire-feed additive layer manufacturing (ALM). Materials Science and Engineering: A, 532, pp.295-307.
25. Tang, H.P., Qian, M., Liu, N., Zhang, X.Z., Yang, G.Y. and Wang, J., 2015. Effect of powder reuse times on additive manufacturing of Ti-6Al-4V by selective electron beam melting. Jom, 67(3), pp.555-563.
26. Le Bourhis, F., Kerbrat, O., Dembinski, L., Hascoet, J.Y. and Mognol, P., 2014. Predictive model for environmental assessment in additive manufacturing process. Procedia CiRP, 15, pp.26-31.
27. Bhavar, V., Kattire, P., Patil, V., Khot, S., Gujar, K. and Singh, R., 2014, September. A review on powder bed fusion technology of metal additive manufacturing. In 4th International Conference and Exhibition on Additive Manufacturing Technologies-AM-2014, September (pp. 1-2).

28. Lagutkin, S., Achelis, L., Sheikhaliev, S., Uhlenwinkel, V. and Srivastava, V., 2004. Atomization process for metal powder. Materials Science and Engineering: A, 383(1), pp.1-6.
29. Pinkerton, A.J. and Li, L., 2005. Direct additive laser manufacturing using gas-and water-atomised H13 tool steel powders. The International Journal of Advanced Manufacturing Technology, 25(5-6), pp.471-479.
30. Witzel, J., Kelbassa, I., Gasser, A. and Backes, G., 2010, September. Increasing the deposition rate of Inconel 718 for LMD. In International Congress on Applications of Lasers & Electro-Optics (Vol. 2010, No. 1, pp. 304-310). LIA.
31. Aldrich, R., 2000. Laser fundamentals.
32. Ding, K. and Ye, L., 2006. Laser shock peening: performance and process simulation. Woodhead Publishing.
33. Mahamood, R.M. and Akinlabi, E.T., 2017. Scanning speed influence on the microstructure and micro hardness properties of titanium alloy produced by laser metal deposition process. Materials today: Proceedings, 4(4), pp.5206-5214.
34. Konert, M. and Vandenberghe, J.E.F., 1997. Comparison of laser grain size analysis with pipette and sieve analysis: a solution for the underestimation of the clay fraction. Sedimentology, 44(3), pp.523-535.
35. Vigneau, E., Loisel, C., Devaux, M.F. and Cantoni, P., 2000. Number of particles for the determination of size distribution from microscopic images. Powder Technology, 107(3), pp.243-250.
36. Eshel, G., Levy, G.J., Mingelgrin, U. and Singer, M.J., 2004. Critical evaluation of the use of laser diffraction for particle-size distribution analysis. Soil Science Society of America Journal, 68(3), pp.736-743.
37. Zhang, Y., Xi, M., Gao, S. and Shi, L., 2003. Characterization of laser direct deposited metallic parts. Journal of materials processing technology, 142(2), pp.582-585.
38. Huang, Y.L., Liu, J., Ma, N.H. and Li, J.G., 2006. Three-dimensional analytical model on laser-powder interaction during laser cladding. Journal of Laser Applications, 18(1), pp.42-46.
39. Fu, Y., Loredo, A., Martin, B. and Vannes, A.B., 2002. A theoretical model for laser and powder particles interaction during laser cladding. Journal of Materials Processing Technology, 128(1-3), pp.106-112.
40. Parr, R.G. and Pearson, R.G., 1983. Absolute hardness: companion parameter to absolute electronegativity. Journal of the American Chemical Society, 105(26), pp.7512-7516.
41. Arrizubieta, J.I., Lamikiz, A., Cortina, M., Ukar, E. and Alberdi, A., 2018. Hardness, grainsize and porosity formation prediction on the Laser Metal Deposition of AISI 304 stainless steel. International Journal of Machine Tools and Manufacture, 135, pp.53-64.

42. Pinkerton, A.J., 2015. Advances in the modeling of laser direct metal deposition. Journal of laser applications, 27(S1), p.S15001.
43. Sastry, S.K., 2013. Chemical and bioprocess engineering: fundamental concepts for first-year students. New York, NY: Springer.
44. Dr. R.K.bansal ,"A text book of fluid mechanics & hydraulic machines"ninth edition. ISBN: 9788131808153
45. Kumar, S., Sharma, V., Choudhary, A.K.S., Chattopadhyaya, S. and Hloch, S., 2013. Determination of layer thickness in direct metal deposition using dimensional analysis. The International Journal of Advanced Manufacturing Technology, 67(9-12), pp.2681-2687.
46. Sonin, A.A., 2004. A generalization of the Π-theorem and dimensional analysis. Proceedings of the National Academy of Sciences, 101(23), pp.8525-8526.
47. Oehlert, G.W., 2010. A first course in design and analysis of experiments.
48. Hanrahan, G. and Lu, K., 2006. Application of factorial and response surface methodology in modern experimental design and optimization. Critical Reviews in Analytical Chemistry, 36(3-4), pp.141-151.
49. Nokoe, S., 1992. Technical paper 7: Statistical and experimental design considerations in alley farming. The AFNETA alley farming training manual. BR Tripathi, PJ Psychas (eds.). International Livestock Centre for Africa, Addis Ababa, pp.1-34.
50. Anderson, V.L. and McLean, R.A., 2018. Design of experiments: a realistic approach. Routledge.
51. Roy, R.K., 2001. Design of experiments using the Taguchi approach: 16 steps to product and process improvement. John Wiley & Sons.
52. Sun, Y. and Hao, M., 2012. Statistical analysis and optimization of process parameters in Ti6Al4V laser cladding using Nd: YAG laser. Optics and Lasers in Engineering, 50(7), pp.985-995.
53. Li, Y.X., Zhang, P.F., Bai, P.K., Zhao, Z.Y. and Liu, B., 2018. Analysis of Geometrical Characteristics and Properties of Laser Cladding 85 wt.% Ti+ 15 wt.% TiBCN Powder on 7075 Aluminum Alloy Substrate. Materials, 11(9), p.1551.
54. Lee, E.M., Shin, G.Y., Yoon, H.S. and Shim, D.S., 2017. Study of the effects of process parameters on deposited single track of M4 powder based direct energy deposition. Journal of Mechanical Science and Technology, 31(7), pp.3411-3418.
55. Liu, H., Qin, X., Huang, S., Hu, Z. and Ni, M., 2018. Geometry modeling of single track cladding deposited by high power diode laser with rectangular beam spot. Optics and Lasers in Engineering, 100, pp.38-46.
56. Liu, S. and Kovacevic, R., 2014. Statistical analysis and optimization of processing parameters in high-power direct diode laser cladding. The International Journal of Advanced Manufacturing Technology, 74(5-8), pp.867-878.

57. Saqib, S., Urbanic, R.J. and Aggarwal, K., 2014. Analysis of laser cladding bead morphology for developing additive manufacturing travel paths. Procedia Cirp, 17, pp.824-829.
58. Manonmani, K., Murugan, N. and Buvanasekaran, G., 2007. Effects of process parameters on the bead geometry of laser beam butt welded stainless steel sheets. The International Journal of Advanced Manufacturing Technology, 32(11-12), pp.1125-1133.
59. Davim, J.P., Oliveira, C. and Cardoso, A., 2006. Laser cladding: an experimental study of geometric form and hardness of coating using statistical analysis. Proceedings of the Institution of Mechanical Engineers, Part B: Journal of Engineering Manufacture, 220(9), pp.1549-1554.
60. De Oliveira, U., Ocelik, V. and De Hosson, J.T.M., 2005. Analysis of coaxial laser cladding processing conditions. Surface and Coatings Technology, 197(2-3), pp.127-136.
61. Sarkar, A., 2018. Interactive analytical modelling (No. UCAM-CL-TR-920). University of Cambridge, Computer Laboratory.
62. Picasso, M., Marsden, C.F., Wagniere, J.D., Frenk, A. and Rappaz, M., 1994. A simple but realistic model for laser cladding. Metallurgical and Materials Transactions B, 25(2), pp.281-291.
63. Liu, J. and Li, L., 2005. Effects of powder concentration distribution on fabrication of thin-wall parts in coaxial laser cladding. Optics & Laser Technology, 37(4), pp.287-292.
64. Pinkerton, A.J., 2007. An analytical model of beam attenuation and powder heating during coaxial laser direct metal deposition. Journal of Physics D: Applied Physics, 40(23), p.7323.
65. Pinkerton, A.J. and Li, L., 2002. A verified model of the behaviour of the axial powder stream concentration from a coaxial laser cladding nozzle. In Proceedings of ICALEO (Vol. 2).
66. Liu, J., Li, L., Zhang, Y. and Xie, X., 2005. Attenuation of laser power of a focused Gaussian beam during interaction between a laser and powder in coaxial laser cladding. Journal of Physics D: Applied Physics, 38(10), p.1546.
67. Toyserkani, E., Corbin, S. and Khajepour, A., 2005. Laser Cladding CRC Press. Boca Raton, Florida.
68. Diniz Neto, O.O., Alcalde, A.M. and Vilar, R., 2007. Interaction of a focused laser beam and a coaxial powder jet in laser surface processing. Journal of Laser Applications, 19(2), pp.84-88.
69. Haider, A. and Levenspiel, O., 1989. Drag coefficient and terminal velocity of spherical and nonspherical particles. Powder technology, 58(1), pp.63-70.
70. El Cheikh, H., Courant, B., Branchu, S., Hascoet, J.Y. and Guillén, R., 2012. Analysis and prediction of single laser tracks geometrical characteristics in coaxial laser cladding process. Optics and Lasers in Engineering, 50(3), pp.413-422.

71. Ahn, D.G., 2011. Applications of laser assisted metal rapid tooling process to manufacture of molding & forming tools—state of the art. International Journal of Precision Engineering and Manufacturing, 12(5), pp.925-938.
72. Toyserkani, E., Khajepour, A. and Corbin, S.F., 2004. Laser cladding. CRC press.
73. Toyserkani. E and Khajepour. A., 2005, “Laser Cladding” CRC Press, LLC, Boca Raton, Florida, pages 280.
74. Tabernero. I, Lamikiz. A and Ukar. E., 2014, “Modeling of the geometry built-up by coaxial laser material deposition process.” Int. J. of Advanced Manuf Technology, vol.70, pp. 843- 851
75. Hou, G.; An, Y.; Zhao, X.; Zhou, H.; Chen, J.; Li, S.; Deng, W. Improving interfacial, mechanical and tribological properties of alumina coatings on Al alloy by plasma arc heat-treatment of substrate. Appl. Surf. Sci. 2017, 411, 53–66
76. Mazumder, J., Morgan, D. and Skszek, T., POM Group, 2002. Fabrication of biomedical implants using direct metal deposition. U.S. Patent Application 09/916,976.
77. Barrow, J.D., 1983. Dimensionality. Phil. Trans. R. Soc. Lond. A, 310(1512), pp.337-346
78. Bansal, R.K., 1998. A Text Book of Fluid Mechanics and Hydraulic Machines: In MKS and SI Units. Laxmi Publications.
79. Temple, G.F.J., 1952. The accuracy of Rayleigh’s method of calculating the natural frequencies of vibrating systems. Proceedings of the Royal Society of London. Series A. Mathematical and Physical Sciences, 211(1105), pp.204-224.
80. Azam, F.I., Rani, A.M.A., Altaf, K., Rao, T.V.V.L.N. and Zaharin, H.A., 2018, March. An In-Depth Review on Direct Additive Manufacturing of Metals. In IOP Conference Series: Materials Science and Engineering (Vol. 328, No. 1, p. 012005). IOP Publishing
81. Mahmood, K. and Pinkerton, A.J., 2013. Direct laser deposition with different types of 316L steel particle: a comparative study of final part properties. Proceedings of the Institution of Mechanical Engineers, Part B: Journal of Engineering Manufacture, 227(4), pp.520-531.
82. Liu, S. and Kovacevic, R., 2014. Statistical analysis and optimization of processing parameters in high-power direct diode laser cladding. The International Journal of Advanced Manufacturing Technology, 74(5-8), pp.867-878.
83. Gary W. Oehlert University of Minnesota, ‘A First Course in Design and Analysis of Experiments’.
84. V.S.K. Manikanta1, B. Partha Saradhi2, V. Vikram3, Seshank Harsha Chaganti4, Salakapurapu Raghavendra Kumar5 “Application of DOE and ANOVA on Nozzle” International Journal for Research in Applied Science & Engineering Technology (IJRASET)ISSN: 2321-9653; IC Value: 45.98; Volume 6 Issue I, January 2018- Available at www.ijraset.com

85. Montgomery, D.C., Peck, E.A. and Vining, G.G., 2012. Introduction to linear regression analysis (Vol. 821). John Wiley & Sons.
86. Faul, F., Erdfelder, E., Buchner, A. and Lang, A.G., 2009. Statistical power analyses using G* Power 3.1: Tests for correlation and regression analyses. Behavior research methods, 41(4), pp.1149-1160.
87. Singh, G., Pai, R.S. and Devi, V.K., 2012. Response surface methodology and process optimization of sustained release pellets using Taguchi orthogonal array design and central composite design. Journal of advanced pharmaceutical technology & research, 3(1), p.30.
88. Akar Sen, G., 2016. Application of full factorial experimental design and response surface methodology for chromite beneficiation by Knelson concentrator. Minerals, 6(1), p.5
89. Jennings, B.R. and Parslow, K., 1988. Particle size measurement: the equivalent spherical diameter. Proceedings of the Royal Society of London. A. Mathematical and Physical Sciences, 419(1856), pp.137-149.
90. Fundamentals of Modern Manufacturing, Materials,Processes,andSystems, Mikell P. Groover, Fourth Edition

CERTIFICATE OF COMPLETENESS

It is hereby certified that the dissertation submitted by *NS Amna Liaqat*, Registration No.*00000172417*, Titled: "*Modeling the effect of non-spherical particle size in laser metal deposition process"* has been checked/reviewed and its contents are complete in all respects.

Signature of Supervisor
(Dr. Khalid Mahmood)